

#121

## FINAL REPORT (8/1/94-12/31/97)

Contract No. DE-FG22-94PC94215

Project Title: Conversion of Coal Wastes into Waste-Cleaning Materials

Principal Investigator: Wei-Heng Shih

Graduate Student: Hsiao-Lan Chang

### INTRODUCTION

Each year 850 million tons of coal are used in the United States and the ash generated amounts to 50 million tons. The disposal of the large amount of fly ash is a pressing problem because of shortage of landfill sites. Other than landfill, fly ash has been used as a filler for roadway foundation, landfill cover, and replacement for cement. However, due to the large amount of fly ash generated, new ways of utilizing fly ash are needed. Recently, several authors showed that zeolites can be synthesized by treating fly ash with NaOH.<sup>1-7</sup> Due to their uniform molecular pore sizes and large surface areas, zeolites are very useful materials with a wide range of applications such as molecular sieves, adsorbents, and catalysts.<sup>8</sup> The conversion of fly ash into zeolites not only eliminates the disposal problem but also turns an otherwise waste material into a useful one.

In the beginning part of this project, we successfully converted the fly ash from the Eddystone plant of PECO Energy into faujasites and zeolite A. However, when we used the same approach to convert ashes from other power plants, it was not successful. Because of the differences in chemical compositions between different ashes, the conversion process has to be modified. Therefore the first goal in this project is to find a general method that can convert ashes of a wide variety of chemical compositions into zeolites. The zeolites synthesized from fly ash are then studied for their ion exchange behavior for the application in removing heavy metal ions from waste streams.

In an attempt to broaden the applications of fly ash, investigation into the formation of mesoporous materials from fly ash was initiated. Mesoporous materials were discovered three years ago by scientists at Mobil<sup>9</sup> and have been under active research by many researchers since then. Mesoporous materials have large surface areas with variable pore sizes in the range of  $>20$  Å. Potential applications of mesoporous materials include catalysts, adsorbents, molecular sieves, etc.<sup>10</sup> If mesoporous materials can be converted from fly ash, it will open up another area of applications for fly ash. The second goal of this project is to convert fly ash into mesoporous materials.

The project was started in August 1, 1994. Mr. Hsiao-Lan Chang, who has a master degree from University of Maryland previously, came from Taiwan and started working August 1. Mr. Chang mainly worked on the conversion of fly ash into zeolites and mesoporous materials. He did an outstanding job in completing these two parts of work. Hsiao-Lan obtained his PhD degree in September of 1997.

In this project, we purchased the Quantachrome NOVA 2200 Surface Area and Pore Size Analyzer for the characterization of the zeolites and mesoporous materials synthesized from fly ashes.

In the following, I will divide the description of our results in three sections: synthesis of zeolites from fly ash, applications of treated fly ash, and mesoporous materials from fly ash.

## **DISCLAIMER**

This report was prepared as an account of work sponsored by an agency of the United States Government. Neither the United States Government nor any agency thereof, nor any of their employees, make any warranty, express or implied, or assumes any legal liability or responsibility for the accuracy, completeness, or usefulness of any information, apparatus, product, or process disclosed, or represents that its use would not infringe privately owned rights. Reference herein to any specific commercial product, process, or service by trade name, trademark, manufacturer, or otherwise does not necessarily constitute or imply its endorsement, recommendation, or favoring by the United States Government or any agency thereof. The views and opinions of authors expressed herein do not necessarily state or reflect those of the United States Government or any agency thereof.

## **DISCLAIMER**

**Portions of this document may be illegible  
in electronic image products. Images are  
produced from the best available original  
document.**

Contract No. DE-FG22-94PC94215

Project Title: Conversion of Coal Wastes into Waste-Cleaning Materials

Principal Investigator: Wei-Heng Shih

Graduate Student: Hsiao-Lan Chang

## INTRODUCTION

Each year 850 million tons of coal are used in the United States and the ash generated amounts to 50 million tons. The disposal of the large amount of fly ash is a pressing problem because of shortage of landfill sites. Other than landfill, fly ash has been used as a filler for roadway foundation, landfill cover, and replacement for cement. However, due to the large amount of fly ash generated, new ways of utilizing fly ash are needed. Recently, several authors showed that zeolites can be synthesized by treating fly ash with NaOH.<sup>1-7</sup> Due to their uniform molecular pore sizes and large surface areas, zeolites are very useful materials with a wide range of applications such as molecular sieves, adsorbents, and catalysts.<sup>8</sup> The conversion of fly ash into zeolites not only eliminates the disposal problem but also turns an otherwise waste material into a useful one.

In the beginning part of this project, we successfully converted the fly ash from the Eddystone plant of PECO Energy into faujasites and zeolite A. However, when we used the same approach to convert ashes from other power plants, it was not successful. Because of the differences in chemical compositions between different ashes, the conversion process has to be modified. Therefore the first goal in this project is to find a general method that can convert ashes of a wide variety of chemical compositions into zeolites. The zeolites synthesized from fly ash are then studied for their ion exchange behavior for the application in removing heavy metal ions from waste streams.

In an attempt to broaden the applications of fly ash, investigation into the formation of mesoporous materials from fly ash was initiated. Mesoporous materials were discovered three years ago by scientists at Mobil<sup>9</sup> and have been under active research by many researchers since then. Mesoporous materials have large surface areas with variable pore sizes in the range of  $>20 \text{ \AA}$ . Potential applications of mesoporous materials include catalysts, absorbents, molecular sieves, etc.<sup>10</sup> If mesoporous materials can be converted from fly ash, it will open up another area of applications for fly ash. The second goal of this project is to convert fly ash into mesoporous materials.

The project was started in August 1, 1994. Mr. Hsiao-Lan Chang, who has a master degree from University of Maryland previously, came from Taiwan and started working August 1. Mr. Chang mainly worked on the conversion of fly ash into zeolites and mesoporous materials. He did an outstanding job in completing these two parts of work. Hsiao-Lan obtained his PhD degree in September of 1997.

In this project, we purchased the Quantachrome NOVA 2200 Surface Area and Pore Size Analyzer for the characterization of the zeolites and mesoporous materials synthesized from fly ashes.

In the following, I will divide the description of our results in three sections: synthesis of zeolites from fly ash, applications of treated fly ash; and mesoporous materials from fly ash.

9/1/94 11:00:15

9/1/94 11:00:15

## 1.1 Synthesis of Zeolites from As-Received Fly Ash

### 1.1.1 Experimental Procedures

As-received fly ash was mixed with 2.8 M sodium hydroxide solution at room temperature in a 250 ml plastic bottle. The weight ratio of sodium hydroxide solution to fly ash was equal to 2.5. The mixture was aged at room temperature and ambient pressure with stirring for 2 days and cured at  $38\pm1^{\circ}\text{C}$  in a glass flask with a rubber stopper. To increase the amount of aluminum in some mixtures of fly ash and sodium hydroxide, 13.96 g of aluminum hydroxide hydrate were added to the mixture before aging process. To find the curing temperature required to synthesize zeolites from fly ash, some mixtures without adding aluminum hydroxide hydrate were cured at  $90^{\circ}\text{C}$ . At various curing intervals, samples of the mixtures were withdrawn under stirring, and sediment and solution were separated by centrifugation. The sediment was washed twice with distilled water. After drying at  $80^{\circ}\text{C}$  in air for 12 hours and ground, the powder was studied by XRD.

Also, to acquire quantitative information about the amount of zeolites generated from fly ash, certain amount of pure  $\text{BaTiO}_3$  powder was added to the fly ash solution before hydrothermal process.

### 1.1.2 Results and Discussion

As the XRD intensity of  $\text{BaTiO}_3$  in the solid phase of the fly ash mixture did not vary during hydrothermal process, it is believed that  $\text{BaTiO}_3$  did not dissolve in basic conditions. As a result, the amount of the zeolite produced from fly ash can be monitored during hydrothermal process. The grain size has been obtained by measuring the width of the diffraction curve at an intensity equal to half the maximum intensity. The widths measured for the zeolites formed from fly ash are similar. It indicate that the grain sizes of zeolites generated from fly ash are almost the same. Therefore, the relative amount of zeolites formed can be monitored by measuring the intensity height ratio of the generated zeolite to that of  $\text{BaTiO}_3$ . The peaks used were (110) of  $\text{BaTiO}_3$ , (533) of faujasite, (310) of zeolite P and, the averaged intensity height of (311) and (410) of zeolite A.

When fly ash was mixed with NaOH aqueous solution and was heated at  $38^{\circ}\text{C}$ , faujasite type zeolites formed after three days of curing. Furthermore, based on  $\text{BaTiO}_3$  as an internal standard, the amount of the generated faujasites contained in the slurry as a function of the curing time is shown in Fig.1. It indicates that after five days of curing, the amount of generated faujasites no longer changed; it fluctuated about a constant value. The particle size distribution by volume shows that the treated fly ash has an additional distribution peak relative to the as-received fly ash. It is believed that the additional size distribution peak is due to the formation of faujasites. From the volume percentage of the additional size distribution peak, it was estimated that the amount of the generated zeolite in the fly ash is approximately 20 vol%.

When the fly ash and NaOH mixtures were treated at  $90^{\circ}\text{C}$  rather than  $38^{\circ}\text{C}$ , zeolite P formed. The amount of zeolite P formed at  $90^{\circ}\text{C}$  as a function of the curing time is shown in Fig.1 and indicates that zeolite P formed earlier and the relative intensity ratio of generated zeolite P to  $\text{BaTiO}_3$  was roughly three times that of generated faujasites. The relative ease with which zeolite P was produced is consistent with the fact that zeolite P is a more stable phase than faujasite. Breck<sup>8</sup> has pointed out that faujasite can dissolve in basic solutions and transform into zeolite P.

The XRD pattern of the fly ash treated with aluminum hydroxide hydrate and NaOH aqueous solution at 38°C indicates that zeolite A formed. Furthermore, using BaTiO<sub>3</sub> as an internal standard, the amount of generated zeolite A in the solid phase of the mixture as a function of the curing time is shown in Fig.1. The figure indicates that, after several days of curing, the amount of zeolite A produced from fly ash no longer changed; it fluctuated at a constant value which is about two times as large as the value of the produced faujasites. In the present synthesis, to ensure that there was enough aluminum species in the liquid phase, the amount of aluminum hydroxide hydrate added was such that the bulk Si/Al atomic molar ratio was made equal to 1.35 by assuming that no Al<sub>2</sub>O<sub>3</sub> dissolved from fly ash but all SiO<sub>2</sub> (about 50 wt% in Eddystone ash (I), see Table 1) in fly ash dissolved. This assumption is reasonable since zeolite A can be synthesized in the alkali solution with an excess of aluminate in liquid phase (the bulk Si/Al atomic molar ratio can decrease to 0.12)<sup>11</sup> and the solubility of Al<sub>2</sub>O<sub>3</sub> is lower than that of silicon oxide.<sup>12,13</sup> On the other hand, when the amount of aluminum hydroxide hydrate was added such that the bulk Si/Al=1.35 assuming both silicon species and aluminum species in fly ash dissolved completely, no zeolite A was formed. It is very likely that in this case the bulk Si/Al atomic molar ratio in liquid phase is too high to nucleate zeolite A.

The as-received Eddystone ash consists of spherical particles with a wide range of diameters, as shown in Fig.2. The SEM micrographs of the treated Eddystone ashes containing faujasite and zeolite A are shown in Fig.3 and Fig.4, respectively. Fig.3 shows the generated faujasite particles existing in agglomerates of small, uniform-sized, non-spherical particles. It was difficult to identify the individual faujasite particle for EDXS analysis. The morphology of the treated Eddystone ash containing zeolite A showed some cubic particles with a size of about 1  $\mu\text{m}$  as seen in Fig.4. The EDXS analysis of the individual cubes showed an average Si/Al molar ratio of 1 indicating that they are indeed zeolite A. Furthermore, it was found that the Na/Al ratio is less than 1, which is expected if each Al substitution for Si is compensated by Na, indicating that some Na ions in zeolite A may have been ion-exchanged during the hydrothermal process.

When zeolite A and faujasite were produced from fly ash, the XRD pattern of the solid phase of the mixture showed that there were peaks of quartz and mullite. This indicates that some Al and Si elements of as-received fly ash had not been completely consumed. This is the main reason why the yield of generated zeolites is not high. In an attempt to increase the yield of the zeolite converted from fly ash, a pretreatment of as-received fly ash was investigated as discussed in the following section.

## 1.2 Synthesis of Zeolites from Fly Ash with the Fusion Method

The raw materials used in these experiments were Eddystone ash (II), Goudey ash and Conembaugh ash. The chemical composition of these ashes are shown in Table 1. The crystalline phases are quartz and mullite. In the previous section fly ash has been used as the source of Si and Al to produce zeolites. However, Al and Si contained in mullite and quartz are very difficult to dissolve at 38°C. To increase the yield of generated zeolites from fly ash, a fusion method was developed. The fusion method has been used in the past to decompose inorganic compounds.<sup>14</sup> Shigemoto et al.<sup>4</sup> has previously applied the fusion method to synthesize zeolite X from one fly ash. Sodium compounds, such as NaOH, Na<sub>2</sub>CO<sub>3</sub>, are the typical reagents in a fusion method due to their high reactivity.

### 1.2.1 Experimental Procedures

with NaOH powder in a ball mill. The weight ratio of fly ash to NaOH powder is 1:1.2. After ball milling, the powders were poured into a stainless steel crucible and heated at 550°C in air for 1 hour. To avoid contamination of the powders by the chemical reaction between NaOH and stainless steel, each stainless steel crucible was only used three times and the fused fly ash powders were taken from the center region of the crucible after the heat treatment. The fused fly ash powder was ground in a mortar and pestle and poured into a 250 ml plastic bottle followed by the addition of distilled water. The weight ratio of fused fly ash powder to water was 0.2. The mixture was first aged 1 day with stirring at room temperature and ambient pressure. Some samples were taken out from the sediments separated from the solution by centrifugation, and dried at 80°C for 12 hours in air. These samples were analyzed by XRD to identify the crystalline phases.

Two hydrothermal procedures were carried out for the mixture containing fused fly ash after one-day aging. (1) The mixture was poured into a 250 ml of glass flask with a rubber stopper and cured at 60 and 90°C at ambient pressure, respectively. At various curing intervals, the supernatant was collected by centrifuging the mixture. 1 ml of the supernatant was diluted with 49 ml distilled water and analyzed by atomic absorption spectroscopy (AAS) to obtain concentrations of the Si, Al and Fe species in the supernatant. At the same curing intervals, some solid samples were recovered from the sediment of the mixture. (2) The supernatant and the sediment of the mixture were separated by centrifugation. The supernatant was decanted into a glass flask with a rubber stopper and cured at 60°C at ambient pressure. Aluminum hydroxide hydrate was added to some flasks of supernatant to increase the Al content and cured at 60°C. The precipitated solid at various curing intervals was recovered by centrifugation. On the other hand, the sediment of the mixture was added with the same amount of distilled water as that of the supernatant of the previous mixture to form the second mixture. The second mixture was aged with stirring for one day at room temperature and was poured into another glass flask with a rubber stopper and cured at 60°C. At various curing intervals, the sediment of the second mixture was collected by centrifugation. All sediments obtained from hydrothermal procedures (1) and (2) were washed two times with distilled water followed by centrifugation to remove the residue of sodium hydroxide and soluble impurities. The solid powder was dried at 80°C in air for 12 hours.

Also to obtain quantitative information about the amount of the generated zeolites from the three fly ashes, certain amount of BaTiO<sub>3</sub> powder was added to the mixture containing fused fly ash before hydrothermal process and the mixture was treated with the hydrothermal procedure (1). The XRD intensity ratio of the (533) peak of the generated faujasite from fly ashes and the (110) peak of the BaTiO<sub>3</sub> powder was used to estimate the amount of generated faujasites in each fused fly ash. At the same time, the relative amount of generated faujasites changes with the curing time and can be monitored by measuring the change of the relative intensity height ratio of the generated zeolites to BaTiO<sub>3</sub> powder.

Besides the XRD pattern, the Si/Al and Na/Al molar ratios are important to determine the type of zeolites formed from fly ash especially for isostructural zeolites, X and Y. The chemical composition of generated zeolites was analyzed by SEM with the EDXS technique. For comparison, the morphology of the commercial zeolite was analyzed and used as the standard image.

### 1.2.2 Results and Discussion

In the previous study without fusion, the peaks of quartz and mullite persisted during hydrothermal process. However, when fly ash was fused with NaOH powder, a large amount of sodium silicate was formed. The XRD pattern of fused fly ash is shown in

quartz and mullite in as-received fly ash have reacted with NaOH to form sodium silicates or amorphous aluminosilicates. When fused fly ash was mixed with distilled water and aged 1 day at room temperature, the XRD pattern of the sediment of the mixture is also shown in Fig.5. There is no crystalline phase in the sediment. This result indicates that the crystalline sodium silicates formed in the fused fly ash have a high solubility and easily dissolve in a basic condition.

When the mixture containing fused fly ash was cured at 60°C, faujasite type zeolite formed. The intensity of these faujasites is higher than that of the faujasite converted from fly ash without fusion as described earlier. This means that the yield of faujasite produced from fly ash with fusion is higher, and all three fly ashes can be used for the formation of faujasite. However, the XRD intensity of faujasites made from the three ashes are different. The reason is due to the fact that the chemical compositions of the three as-received fly ashes are different. As a result the amount of faujasite produced is different. When the mixture was cured at 90°C, zeolite P rather than faujasite was formed.

For the hydrothermal procedure (2), the XRD results of the precipitated solids from the supernatants of the mixtures, using fused Eddystone, Goudey and Conemaugh ashes, showed that the generated zeolites are faujasites. The XRD intensity of faujasites produced from procedure (2) is higher than that of procedure (1) indicate higher percentage of faujasite exist in the samples. The result indicates that the sediment can be repeatedly used to obtain faujasites and the dissolution of Si and Al species still continued in the second mixture.

When 0.4 g aluminum hydroxide hydrate was added to the supernatant, zeolite A formed. This observation indicated the bulk Si/Al ratio in supernatant with the addition of aluminum species was low enough for the nucleation of zeolite A. The generated faujasites discussed in Section 5.3 can not be obtained from the supernatant of the mixture containing as-received fly ash and NaOH aqueous solution, which might be due to a lower amount of silicates and aluminates in the liquid phase. From the formation of zeolites in supernatants, it is believed that the nucleation of zeolite must have occurred in the liquid phase and then precipitate. Although using the supernatant we can synthesize purer faujasites, the amount produced is not large. In fact the amount of faujasites produced from the supernatant is less than that from procedure (1). Because the amount of the precipitates from the supernatants is less than those obtained in hydrothermal procedure (1), the recycled amount of fly ash might be too small to be used in real applications. In the following, we will concentrate on the faujasite produced by hydrothermal procedure (1) unless otherwise noted.

The X-ray diffraction intensity of the faujasites produced from the three fly ashes was measured and related to that of BaTiO<sub>3</sub> at various curing times. The yield of the generated faujasite based on the intensity ratio is shown in Fig.6 as a function of the curing time. Compared with the synthesis method without fusion, the fusion of fly ash before hydrothermal process can be used to produce faujasites from all three fly ashes and also have higher yield as shown in Fig.6. Thus, the fusion method is shown to be a general and efficient method for converting fly ash to faujasites, regardless of the compositional variations of the three fly ashes.

The generality of using different fly ashes as raw materials and the higher yield of faujasites from the fusion method, are due to the fact that more aluminum and silicon ions exist in the liquid phase of the mixture containing fused fly ash. The higher solubility of sodium silicates and amorphous aluminosilicate, which were formed after a chemical reaction of mullite and quartz with NaOH powder during fusion process, increased the concentration of aluminum and silicon ions. The actual concentration of aluminum, silicon

of the Si, Al and Na are shown in Fig.7-9, respectively. From Fig.7 the concentration of Al ion in three fused fly ash solutions decreases with curing time and, becomes negligible after two days of curing. The results of Fig.6 show that the faujasite starts forming after two days of curing. The combined results of Fig.6 and Fig.7 indicate that the formation of faujasite is related to the concentration of aluminum ion in liquid phase. When the amount of aluminum ion decreases to a negligible value, the crystal growth can not continue. Ginter et al.<sup>16</sup> have shown that the formation of Al-rich nuclei during aging is critical to the precipitation of faujasites. They proposed that the Al-rich nuclei transformed to faujasite during heat treatment followed by the addition of Si species to the nuclei. When the Si/Al ratio in the nuclei increases the structure of faujasite forms and grows.

Contrary to the decrease in the concentration of Al ions, the concentrations of Si and Na ions decrease initially and, after two days curing, start to increase and finally reach equilibrium values. These results indicate that large amounts Si and Na species remained in liquid phase. It is known that the synthesis of zeolites from pure chemical precursors always leaves unused silicon species as shown in Fig.8.<sup>15,16</sup> It is concluded from the results of Figs.7-9 that the aluminum ion in the liquid phase is the controlling species in the synthesis of faujasites and higher amount of the aluminum species in the precursor mixture results in larger yields of faujasites. This is consistent with the fact that the yield of the generated faujasite from Conemiaugh ash is greater as shown in Fig.6.

The typical morphology of the generated faujasite from fused Conemiaugh ash mixture (hydrothermal procedure 1) and from the supernatant of the fused Conemiaugh ash mixture (hydrothermal procedure 2) are shown in Fig.10 and Fig.11, respectively. There are many crystallites with facets in Fig.10 which is different from the spherical shape of as-received fly ash particles. Therefore, the individual faujasite particles can be identified from the SEM micrographs and the measurement of the chemical composition in each faujasite particles was obtained by EDXS mode. The Si/Al and Na/Al molar ratios of each faujasite converted from the three fly ashes and UOP ZY-54 are averaged over five different faujasite particles. The results are shown in Table 2. UOP ZY-54 has a higher Si/Al molar ratio than the faujasites generated from the three fly ashes. However, the Si/Al molar ratios of the generated faujasites are similar no matter which fly ash is used as the raw material. The overall molar ratios of Na/Al are close to one in the generated faujasites from the three fly ashes as listed in Table 2. This is consistent with the fact that sodium ion attaches the aluminosilicate network to balance the charge when the tetrahedral Al atom substitutes for the tetrahedral silicon atom.

In the study of Kuehl et al.<sup>17</sup> it was shown that the lattice parameter,  $a_0$ , increases with more aluminum content in the framework of faujasite type zeolites. The lattice parameter of generated faujasites was determined by the XRD method as mentioned by Kuehl et al.<sup>17</sup> The lattice parameter was obtained from the average d-spacing of the (10,10,0) peak; the results are listed in Table 3. The Si/Al ratios of the faujasites generated from fly ash are in the range of zeolite X. The higher Si/Al ratio of UOP ZY-54 indicates UOP ZY-54 is zeolite Y type. The results of Table 3 are similar to those of Table 2 measured by EDXS in SEM. It is observed that the treated Eddystone ash obtained from the low-temperature process without fusion has a smaller Si/Al ratio than the treated ashes with fusion indicating the bulk Si/Al ratio in the supernatant of the Eddystone ash (I) mixture is lower than those of mixtures containing fused fly ashes. It indicated that more Si ions dissolve from the fused fly ash due to the formation of sodium silicates.

## 2. APPLICATIONS OF ZEOLITES CONVERTED FROM FLY ASH

## 2.1 Ion Exchange

### 2.1.1 Experimental Procedures

The ion exchange capabilities of the treated fly ashes with a fusion method by hydrothermal procedure (1) were measured for 0.1 N of cesium ions or cobalt ions at room temperature. All treated fly ashes were washed and dried as experimental procedure A. The ion exchange experiment began with preparing 38 ml of distilled water containing 0.9 g of treated fly ash, in which the pH value was typically 10.5. The treated fly ash mixture was added with 2 ml of 2 N test ions solution and the sodium ion concentration in the liquid phase of the test mixture was measured using a sodium ion probe at various reaction times. As the ion exchange reaction reached equilibrium, the sodium ion concentration in liquid phase would stay at an equilibrium value. Commercial zeolites, UOP X-60 (zeolite X), UOP ZY-54 (zeolite Y), UOP 4A (zeolite A), were tested in the procedures mentioned above. Each mixture after ion exchange experiment were centrifuged and the sediment was dried at 80°C for 12 hours in air. Dried sediments were ground and prepared for the SEM/EDXS analysis.

### 2.1.2 Results and Discussion

When the  $\text{Cs}^+$  or  $\text{Co}^{+2}$  ions exchanged with the  $\text{Na}^+$  ion in the zeolites, the sodium ion concentration in the test mixture would increase to a maximum value where the ion exchange reaction approached the equilibrium. The ion exchange behavior with  $\text{Cs}^+$  ions of commercial zeolites and treated fly ashes containing faujasite is shown in Fig.12. No test was done for commercial zeolite A (UOP4A) because the exchange capability of zeolite A with  $\text{Cs}^+$  ions is low. It is shown from Fig.12 that the concentrations of sodium ions in the liquid phase of test solutions increase with the reaction time for all samples. The ion exchange capability was obtained by the net increase of sodium ion concentration in each liquid phase of the test mixture after 48 hour reaction when the equilibrium was reached. The summary of ion exchange capability is listed in Table 4. Treated Conemiaugh ash has a higher ion exchange capability than the other treated fly ashes and the ion exchange capability of treated Conemiaugh ash is 75.6 % that of UOP X-60.

There are two parameters affecting the ion exchange capability of samples. One is the percentage of zeolites in the treated fly ash; another is the Si/Al ratio of zeolites. Since the zeolites converted from fly ashes and UOP ZY-54 belong to the faujasite type according to the similar XRD pattern, the pore size effect can be neglected. The Si/Al ratios of generated faujasites from three ashes are also similar. Therefore the higher ion exchange capability of treated Conemiaugh ash could be related to the higher percentage of the generated faujasites in the treated Conemiaugh ash, as discussed earlier. Although UOP ZY-54 have a higher Si/Al ratio than generated faujasites, the fact that the ion exchange capability of UOP ZY-54 is higher than that of treated fly ashes is due to its higher purity. The ion exchange capability of UOP X-60 is larger than that of UOP ZY-54. This is due to the smaller Si/Al ratio in the framework of UOP X-60.

After the ion exchange test, the cesium contents in the treated Conemiaugh ash and UOP ZY-54 were determined by EDXS in SEM. The cesium distribution in different parts of the treated Conemiaugh ash is shown in Fig.13. There are some regions with irregular shape where the cesium content is much higher than in the crystallite faujasites, that have the morphology with facets. Since the cesium content in the as-received fly ash is negligibly small, it is believed that the increase of cesium content in the crystallite faujasites of treated fly ashes derives from an ion exchange reaction. Using the cesium content

Conembaugh ash were estimated. The results are shown in Fig.13. The faujasite regions, #2 and #4 as indicated in Fig.13, have a cesium exchange capability in the neighborhood of 1.6 millieq/g, which is close to that listed in Table 4 measured by a sodium probe. The regions #1 and #3 in Fig.13 have much higher cesium contents than faujasite regions so that the cesium exchange capabilities of these regions range from 3.6 to 3.7 millieq/g. It is likely that these regions with high cesium content are areas where  $\text{Cs}^+$  ions reacted with aluminosilicates and precipitated in some form of cesium compound due to the high pH condition. This observation was also indicated by Singer et al.<sup>18</sup> and is consistent with the fact that metal compounds tend to precipitate at alkaline conditions. Therefore, besides the ion exchange reaction, additional cesium may be removed from the liquid phase of test mixtures due to the reaction between cesium and aluminosilicate to form cesium compound precipitates. This observation was also found in UOP ZY-54 after cesium exchange experiments. It was found that most areas of UOP ZY-54 have cesium exchange capabilities in the neighborhood of 1.8 millieq/g, similar to that measured by a sodium probe. At the same time, there were regions with the cesium exchange capability of 4 millieq/g. By using a fusion method, the cesium exchange capability of treated fly ash is similar to that of the synthetic faujasite, and 2.4 times that of treated fly ash faujasite without fusion. Compared with the cesium ion exchange capability of treated fly ash made by Amrhein et al.,<sup>7</sup> the treated fly ash with a fusion method has a cesium ion exchange capability two times larger than their treated fly ash.

The ion exchange behavior with  $\text{Co}^{2+}$  ions of commercial zeolites and treated fly ashes containing faujasite is shown in Fig.14. Because the size of hydrated  $\text{Co}^{2+}$  ion is about one half of the size of  $\text{Cs}^+$  ion (diameter = 0.32 nm),<sup>19</sup> the pore size of zeolite A is large enough for the passage of  $\text{Co}^{2+}$  ions to replace the  $\text{Na}^+$  ions. The cobalt exchange capabilities of all test samples are summarized in Table 5. All cobalt exchange capabilities of treated fly ashes containing faujasites are higher than that of UOP ZY-54 but lower than that of UOP 4A and UOP X-60. Because the hydrated  $\text{Co}^{2+}$  ion can easily pass through the pore and channel of zeolite A and faujasite, it is believed that the reason why the cobalt exchange capability of zeolite A is larger than that of faujasites (zeolite X and Y), shown in Table 3, is that zeolite A have a smaller Si/Al ratio than faujasites.

The cobalt contents in the treated Conembaugh ash and UOP ZY-54 after exchange test were also determined by EDXS in SEM micrographs. The distribution of cobalt in different regions of the treated Conembaugh ash is shown in Fig.15. Using the same procedure for cesium exchange capability calculation, cobalt exchange capabilities were estimated for different regions of treated Conembaugh ash and are listed in Fig.15. The averaged value of ion exchange capability is 3.49 millieq/g, slightly higher than that measured by the sodium probe as shown in Table 5. The theoretical highest cobalt exchange capability is 4.44 millieq/g when all  $\text{Co}^{2+}$  ions in a 40 ml of 0.1 N  $\text{CoCl}_2$  were completely and homogeneously exchanged by 0.9 g samples. The cobalt exchange capability of UOP 4A is 3.95 millieq/g, that is very close to the theoretical value. In Fig.15 there are regions of high cobalt contents in the treated Conembaugh ash and the obtained cobalt exchange capabilities of those regions are larger than the theoretical value. The reason for these high cobalt exchange capabilities is probably due to the precipitation of cobalt aluminosilicate compounds as discussed above. The cobalt exchange capacity of treated Conembaugh ash is about 75.7 % of that of UOP 4A.

## 2.2 Gas Adsorption and Thermal Stability

zeolite P was investigated and the results are shown in Fig.16. The isotherms of all samples containing faujasite type zeolite are similar and belong to the third type isotherm as described by Brunauer et al.<sup>20</sup> Since the adsorbate molecule size is on the order of the micropore of zeolites, there is strong tendencies for zeolites to physisorb the adsorbate at low relative pressures due to the strong potentials that exist around small pores.<sup>21</sup> The amount of adsorbate adsorbed by each sample increases with the order : UOP ZY-54 > treated ash by hydrothermal procedure (2) > treated fly ash by hydrothermal procedure (1). The treated fly ash obtained by hydrothermal procedure (1) is denoted 'solution' in Fig.16; that by hydrothermal procedure (2) is denoted 'supernatant' in Fig.16. The treated fly ash containing zeolite P adsorbed the least amount of adsorbate. The nitrogen gas adsorption behavior of treated fly ash without fusion showed that it adsorbed less adsorbate than the treated ash samples obtained with fusion.

The specific surface area of as-received fly ash, treated fly ash and commercial zeolite was obtained from the result of nitrogen gas adsorption isotherm. As-received fly ashes have very small specific surface area, in the order of  $2\text{--}5\text{ m}^2/\text{g}$ . The specific surface areas of UOP ZY-54 and 4A are about 950 and  $800\text{ m}^2/\text{g}$ , respectively. With the fusion method, the treated fly ashes containing faujasites have specific surface areas ranging from 250 to  $650\text{ m}^2/\text{g}$ , which is dependent on the fly ash used and the hydrothermal procedure.

The summary of specific surface area of samples is listed in Table 6, in which the data of treated fly ash without fusion are listed for the purpose of comparison. For the treated fly ash obtained from Eddystone, Goudey and Conemaugh ashes by hydrothermal procedure (1) is denoted 'solution' in Table 6; that by treatment procedure (2) is denoted 'supernatant' in Table 6. It is clear that the treated fly ash by treatment (2) has a larger specific surface area than that by hydrothermal procedure (1) and this is consistent with the XRD analysis. It is confirmed that the percentage of generated faujasites in treated fly ash by hydrothermal procedure (2) is higher. The specific surface areas of treated fly ashes without fusion are about  $75$  and  $100\text{ m}^2/\text{g}$ , respectively, for the treated fly ash containing zeolite A and faujasite. These results confirmed that the fusion method can increase the amount of zeolites converted from fly ash.

All of the specific surface areas of treated fly ashes with or without fusion are much higher than the  $42\text{ m}^2/\text{g}$  of the treated fly ash studied by Amrhein et al.<sup>7</sup> and this results in the ion exchange capability of treated fly ash is larger than that of Amrhein et al.<sup>7</sup> A maximum surface area of  $94\text{ m}^2/\text{g}$  was found by Lin et al.<sup>5</sup> in their treated fly ash containing zeolite P, which is similar to the value of the treated fly ash by hydrothermal procedure (1) containing zeolite P,  $54.4\text{ m}^2/\text{g}$ . The treated fly ash containing zeolite P do not show high ion exchange capacity with radioactive species although the surface area is high. The main reasons are the exchangeable  $\text{Na}^+$  ion in the framework of zeolite P is less due to its high Si/Al ratio and also the pore size of zeolite P is too small to let larger ions pass through the channels.

For the application in radioactive waste treatment, the thermal stability of treated fly ash containing zeolites is important because the decay of radioactive species will produce heat. For the test of thermal stability, the treated Conemaugh ash containing faujasites was kept in an alumina crucible and heated to  $540^\circ\text{C}$  and  $740^\circ\text{C}$ , respectively, for 7 hours in air. The heated samples were characterized by XRD and nitrogen gas adsorption.

Fig.17. The isotherm of the sample heated at 540°C is similar to that of the as-synthesized faujasite powder although the amount of nitrogen gas adsorbed is slightly less. In contrast, the isotherm of the sample heated at 740°C differs significantly from those of the samples heated at 540°C and the as-synthesized faujasite powder. It is conspicuous that there is little of the nitrogen gas adsorbed by the sample heated at 740°C. This adsorption behavior implies the pores of faujasite have collapsed due to the change of crystal structure. The XRD patterns of faujasite converted from Conemiaugh ash heat treated at 540°, 740°C are shown in Fig.18. The peaks of the generated faujasite disappeared indicating that the faujasite converted from fly ash is thermally stable at 540°C.

### 3. SYNTHESIS OF MESOPOROUS MATERIALS

#### 3.1 Experimental Procedure

The fly ash used in current experiment is class F fly ash from three power plants of PECO Energy Inc. The chemical composition is shown Table 1. The surfactant is cetyltrimethyl ammonium bromide, CTAB. The sodium hydroxide powder is the analytical reagent supplied by Mallinckrodt Inc., in which the impurities are about 2 wt%. Ammonium hydroxide solution is 4.96 N obtained from Aldrich Chemical Co.

As-received fly ash was mixed with NaOH powder at a weight ratio of 1:1.2 by ball milling for 12 hours. The mixture powder was treated with the fusion process as mentioned earlier. After ground by mortar, 8.8 g of fused fly ash was added to 43 ml of distilled water in a 250 ml of plastic bottle. The mixture was aged 1 day with stirring at room temperature and ambient pressure, and then poured into a 250 ml of glass beaker with a rubber stopper to form the so-called fused fly ash solution. The fused fly ash solution was separated to a supernatant and the sediment by centrifugation. The supernatant is denoted solution I. The sediment was added with distilled water that has the same volume as the solution I and formed the second fused fly ash solution. The second fused fly ash solution was aged 1 day again and separated to the sediment and the second supernatant, which is denoted solution II. 1 ml of solution I or II was diluted with 49 ml of distilled water in a 60 ml plastic tube and the concentration of ions such as  $\text{Si}^{4+}$ ,  $\text{Al}^{3+}$  and  $\text{Na}^+$  in these diluted solution I and II is measured by AAS.

0.755 g of surfactant was mixed with 2.265 g distilled water in a 50 ml glass beaker and stirred with magnetic bar for 5 minutes at 38°C. The 25 wt% surfactant solution was added with 0.5 ml  $\text{NH}_4\text{OH}$  followed by addition of 13.85 ml of distilled water and stirred 10 minutes at room temperature. This is called the surfactant solution, which was poured into the solution I and II as mentioned above and stirred for 30 minutes at room temperature. The solution I and II, containing surfactant solution, was hydrothermally cured at 115°C and the saturation temperature at ambient pressure (about 100°C) in a 250 ml boiling flask and topped with a reflux condenser. Solid samples were taken out at various curing times by centrifugation and washed twice with distilled water. The centrifuged sediment was dried at 80°C in air for 12 hours. After grinding, the solid powders were calcined at 540°C in air for 7 hours at 1°C/min. The calcined powders were analyzed by XRD, TEM/EDXS and nitrogen gas adsorption.

#### 3.2 Results and Discussion

Both solution I and solution II, containing surfactant solution, were studied for the formation of mesoporous materials from Conemiaugh ashes. It was found that the MCM-

24 hours and 48 hours, no crystalline phase formed and only a broad peak of the amorphous silicate appeared in the XRD pattern. The incubation time is longer than that of MCM-41 formed from pure chemical precursor solutions. This longer incubation time might be related to the effects of impurities of the fused fly ash. These impurities, anionic metal species, interfere the templating of surfactant molecules in solution. The XRD patterns of the samples after calcination are shown in Fig.19. As shown in Fig.19, three peaks of the sample, obtained at 150 hours of curing, correspond to the d-spacing values of 3.58 nm ( $d_1$ ), 1.96 nm ( $d_2$ ) and 1.82 nm ( $d_3$ ), respectively. The d-spacing ratios of these peaks were calculated and the results are : 0.55 for  $d_2/d_1$ ; 0.51 for  $d_3/d_1$ . From the d-spacing ratios, the peaks with the d-spacing of 3.58 nm, 1.96 nm and 1.82 nm were identified as the (100), (110) and (200) peaks of typical MCM-41 materials. The XRD patterns of higher angles ( $2\theta > 11^\circ$ ) was measured and indicated that besides the MCM-41 phase there are amorphous silicates coexisting in the samples.

In contrast, no MCM-41 phase was formed from solution I even after 150 hours of curing. The reason why MCM-41 phase did not form in solution I or was less stable than that formed in solution II was analyzed by the ion concentrations in solution I and II.

Before the addition of the surfactant solution, the concentrations  $\text{Si}^{4+}$ ,  $\text{Al}^{3+}$  and  $\text{Na}^+$  ions in solution I and II prepared from Conembaugh ash were obtained by Atomic Absorption Spectroscopy and the results are listed in Table 7. There are significant differences in the Si and Al concentrations between solution I and II. However, it has been shown by our earlier work that the MCM-41 materials can be formed at the bulk Si/Al molar ratio in solution ranging from 1.35 to 200. Therefore, it is concluded that the difference in the Si/Al ratios does not affect MCM-41 synthesis.

Solution I has a sodium ion concentration almost five times larger than that of solution II. The higher NaOH amount in the precursor solutions favored the formation of zeolites,<sup>22</sup> and the sodium ion dominated the synthesis route of aluminosilicate precursor toward the formation of zeolites, which is confirmed by the formation of zeolite P only in solution I and not in solution II. This excess sodium ions might hinder the formation path of the MCM-41 phase because the templating function by surfactant molecules was prevented. The MCM-41 phase was synthesized in conditions of low sodium content or no sodium used, reported by many researchers. It is important that the fusion of fly ash with NaOH for the formation of mesoporous materials. In previous experiments there was no mesoporous materials formed in the solutions of as-received fly ash mixed with NaOH aqueous solution and different amounts of surfactants. It is believed the higher concentration of silicon and aluminum species in the fused fly ash solution promote the formation of mesoporous materials.

The nitrogen adsorption/desorption isotherms for the MCM-41 phase obtained from solution II prepared from Conembaugh ash and cured at 115°C for 150 hours is shown in Fig.20. There is a sharp increase of slope on the adsorption/desorption curve. The flat point of the curve occurs at the value of the relative pressure,  $P/P_0$  corresponding to 0.25. The specific surface area is 735  $\text{m}^2/\text{g}$ , obtained by multipoint BET method. The pore size distribution was calculated by BJH method, and the pore size is quite uniform. The pore size distribution is showed in Fig.21 and the average pore size is about 2.74 nm. Using the  $d_{100}$  spacing of 3.58 nm obtained from the XRD pattern, Fig.18, the lattice constant of the hexagonal pattern is equal to:  $a_0 = (4/3)^{1/2} d_{100} = 4.1 \text{ nm}$ . Therefore, the wall thickness between pores was estimated to be 1.4 nm.

in Fig.22. In this TEM micrograph, a large piece of plate is embedded with particles and fibrils. When focused on the plate region at a higher magnification the pores were orderly distributed in an clearly hexagonal pattern, showed in Fig.23. The size of the pores and the wall thickness between the pores slightly varies in different locations of the TEM micrograph. These variations might correspond to the different projection angles in different regions. The pores could be dark or bright images in TEM micrograph by changing the focus length. From the TEM analysis, the MCM-41 phase occupies about 40-50 % of the total area of the TEM micrograph. The lattice constants of hexagonal patterns at various locations of the TEM micrograph were measured and the average lattice constant was equal to 3.95 nm, which is slightly less than the lattice constant value of 4.1 nm obtained from XRD pattern.

Chemical composition of the different locations in Fig.22 was obtained by EDXS analysis and the results are summarized in Table 8. The MCM-41 aluminosilicates have an average contents of Si=31.21 atom%, Al=2.33 atom%, Fe=0.28 atom% and small amounts of Ca, K, S and P. The data were averaged from 10 locations taken from 3 different plates. An interesting observation is that there is not detectable sodium content in the MCM-41 phase, fibrils and particles and it indicates that most of the sodium ions stay in the supernatant. The Si/Al molar ratio of the MCM-41 aluminosilicates is 13.4 which is much higher than the Si/Al=1.77 in the as-received fly ash. Before the addition of the surfactant solution, the Si/Al molar ratio in the supernatant of the second fused fly ash solution was estimated to be less than 8.3 according to Table 7. Apparently the dissolution of silicates is more efficient than that of aluminum species during aging. The abundance of Si content in the fused fly ash can be seen from the high sodium silicate peaks in XRD pattern of the fused fly ash powder. During the hydrothermal process, the silicon species is more active than aluminum species to participate in the formation of MCM-41 phase. The MCM-41, fibrils and particles all precipitated from the supernatant of the mixture of the second fused fly ash solution and surfactant solution, and have higher Si/Al ratios than the supernatant of the second fused fly ash solution.

Decreasing the Si/Al molar ratio in the MCM-41 phase has been a main concern by many scientists. Previously, Chen et al.<sup>23</sup> showed that MCM-41 phase can be prepared with a Si/Al ratio as low as 29 without observing the presence of octahedral aluminum. Since then there were publications<sup>22,24,25</sup> indicated the formation MCM-41 with Si/Al ratios lower than 29. It is not clear from these publications that MCM-41 aluminosilicates actually have lower Si/Al molar ratios since no direct chemical analysis was done on these samples. It is possible that the samples contained alumina particles, with a tetrahedral connection of aluminum atoms, segregated from Si-rich MCM-41 aluminosilicates. Therefore, the actual Si/Al ratio in the MCM-41 phase is higher than that of these samples. The results of TEM/EDXS, showed in Fig.23, provide the first direct evidence that the MCM-41 aluminosilicates with the Si/Al = 13.4 has been synthesized.

To check the chemical homogeneity of the MCM-41 phase, the standard deviation in the Si/Al ratio from ten locations of the plates in TEM micrograph were measured and equal to 1.1%. This very small standard deviation value indicates that the Si/Al ratio is quite uniform throughout the sample. The MCM-41 aluminosilicates have been converted from fly ash with CTAB surfactant, and the Si/Al molar ratio in this MCM-41 phase is directly identified as low as 13.4. It is conceivable that with the recent results of the MCM-41 formation of pure alumina using dodecyl sulfate<sup>26</sup> or carboxylic acids as surfactant,<sup>27</sup> that MCM-41 aluminosilicates with even lower Si/Al ratios can be made with suitable surfactants. The fact that MCM-41 can be synthesized from fly ash indicates that the impurities in the fly ash are not detrimental to the formation of MCM-41.

To investigate the thermal resistance of generated MCM-41 materials from fly ash, the calcined powder, obtained from solution II of the fused Conemaugh ash after 8 days of curing in a 250 ml boiling flask and topped with a reflux condenser, was treated at 740 and 940°C for 7 hours in air. The XRD patterns of treated samples show that the peaks of MCM-41 materials disappear when samples were heated at 940°C. The nitrogen gas adsorption isotherms of treated samples at different temperatures are shown in Fig.24. Consistent with the XRD results, the gas adsorption of the sample treated at 940°C decreases a lot. The generated MCM-41 materials from fly ash can persist above 740°C, that is similar to the thermal stability of MCM-41 synthesized from pure chemical precursor.

The acid test was performed on the MCM-41 materials as well. The MCM-41 materials converted from fly ash were poured into a 500 ml beaker containing 1 N of hydrogen chloride solution for 1 day at room temperature. The pH value of the solution was less than 1. The sediment of the solution after centrifugation was dried at 80°C for 12 hours in air and analyzed by XRD. The typical XRD pattern of the sediment is shown in Fig.25. The peaks of MCM-41 materials remain indicating the MCM-41 is acid resistant. For the purpose of comparison, the XRD pattern of the commercial zeolite, UOP ZY-54, after acid test of the same procedures is shown in Fig.24 and clearly the structure of the zeolite breaks down. This strong acid resistance of MCM-41 materials is a major advantage over zeolites.

## 4. CONCLUSIONS

### 4.1 Zeolites converted from fly ash

(i) Zeolites have been successfully converted from fly ash. Zeolite A and faujasite are metastable phases and were synthesized at lower temperatures; zeolite P can be formed at higher temperatures since it is a more stable phase.

(ii) The fusion method can convert different fly ashes to zeolites because larger amount of Si and Al can be dissolved from fly ash. The silicon and aluminum species in fly ash reacted with NaOH to form sodium silicates and amorphous aluminosilicates that have high solubility in water. It is shown that Al controls the formation of faujasites and the higher Al content in solutions produces a higher percentage of the generated faujasite in treated fly ash.

(iii) The treated fly ashes with/without fusion all have larger ion exchange capability than as-received fly ash. The highest  $\text{Cs}^+$  ion exchange capability of the treated Conemaugh ash by fusion is about 75.6% of that of commercial zeolite X, UOP X-60; the highest  $\text{Co}^{2+}$  ion exchange capability of the treated Conemaugh ash by fusion is about 75.7% of that of commercial zeolite A, UOP 4A.

(iv) The ion exchange capability of zeolites depends on the Si/Al molar ratio in their framework. The Si/Al molar ratio of the generated faujasites from the fusion method is larger than that of the faujasites produced without the fusion process. It is believed that the fusion method increases the amount of Si species in the solution due to the reaction between silicon species in fly ash and NaOH.

Mesoporous aluminosilicates with uniform pore size can be synthesized from fly ash using the fusion method. The mesopores obtained arrange in an orderly hexagonal pattern. The TEM/EDXS shows the Si/Al molar ratio in the mesoporous materials is 13.4. Also, TEM/EDXS indicates there is no Na contained in the framework of mesoporous materials.

## REFERENCES

1. A. Yoshida and K. Inoue, *Zeolites*, **1986**, 6, 467.
2. T. Henmi *Clay Science* **1987**, 6, 277.
3. J. L. LaRosa, S. Kwan, M. W. Grutzeck, *J. Am. Ceram. Soc.*, **1992**, 75, 1574.
4. N. Shigemoto, H. Hayashi, K. Miyaura, *J. Mater. Sci.* **1993**, 28, 4781.
5. C. -F. Lin, H. - C. Hsi *Environmental Science & Technology* **1995**, 29, 1109.
6. W.-H. Shih, H.-L. Chang, and Z. Shen, *Mater. Res. Soc. Symp. Proc.*, **1995**, 371, 39.
7. C. Amrhein, G. H. Haghnia, T. S. Kim, P. A. Mosher, R. C. Gagajena, T. Amanios, L. Torre, *Environmental Science & Technology* **1996**, 30, 735.
8. D. W. Breck, *Zeolite molecular sieves*, **1974**, John Wiley & Sons, Inc. New York.
9. J. S. Beck, J. C. Vartuli, W. J. Roth, M. E. Leonowicz, C. T. Kresge, K. D. Schmitt, C. T-W. Chu, D. H. Olson, E. W. Sheppard, S. B. McCullen, J. B. Higgins, J. L. Schlenker *J. Am. Chem. Soc.* **1992**, 114, 10834.
10. X. S. Zhao, G. Q. Lu, and G. J. Millar, *Ind. Eng. Chem. Res.*, **1996**, 35, 2075.
11. J. Ceric, *Colloid Interface Sci.*, **1968**, 28, 315.
12. P. Catalfamo, F. Corigliano, P. Primerano, S.D. Pasquale, *Chem. Soc. Faraday Trans.*, **1993**, 89(1), 171.
13. R. H. Mariner, R. C. Surdam *Science* **1970**, 170, 977.
14. W.F. Hillebrand, G.E.F. Lundell, H.A. Bright, J.I. Hoffman, *Applied Inorganic Analysis*, 2nd ed. Wiley, New York, **1962**
15. R.M. Barrer FRS, *Hydrothermal chemistry of zeolites*, **1982**, Academic Press, New York.
16. D. M. Ginter, A. T. Bell, C. J. Radke *Zeolites* **1992**, 12, July/August, 742.
17. G.H. Kuehl, D.H. Olson and E. Dempsey, *J. Phys. Chem.*, **1969**, 78, 387.
18. A. Singer, V. Berkgaot *Environmental Science & Technology* **1995**, 29, 1748
19. J.E. Huheey, E.A. Keiter, R.L. Keiter, *Inorganic Chemistry-Principles of Structure and Reactivity*, 4th Edn, Harper Collins, New York, **1993**, p.114.
20. S. Brunauer, P. Emmett and E. Teller, *J. Am. Chem. Soc.*, **1938**, 60, 309.
21. S. Lowell, *Introduction to Powder Surface Area*, John Wiley And Sons, New York, **1979**
22. R. B. Borade, A. Clearfield *Catalysis Letters* **1995**, 31, 267.
23. C.Y. Chen, H.Y. Li, M.E. Davis, *Microporous Mater.*, **1993**, 2, 27.
24. M. Busio, J. JNnchen, J. H. C. van Hooff *Microporous Materials* **1995**, 5, 211.
25. Z. Luan, C.-F. Cheng, W. Zhou, J. Klinowski, *J. Phys. Chem.*, **1995**, 99, 1018.
26. M. Yada, M. Machida, T. Kijima, *Chem. Comm.* **1996**, 769.
27. F. Vaudry, S. Khodabandeh, M.E. Davis, *Chem. Mater.*, **1996**, 8, 1451.

Table 1. Chemical composition (weight %) of as-received fly ashes.

	SiO <sub>2</sub>	Al <sub>2</sub> O <sub>3</sub>	Fe <sub>2</sub> O <sub>3</sub>	Na <sub>2</sub> O	K <sub>2</sub> O	CaO	Others*
Eddystone (I)	51.57	28.99	10.56	0.46	2.58	3.36	2.48
Eddystone (II)	65.42	28.23	2.14	0.64	0.26	1.72	1.59
Goudey	67.17	20.41	4.07	0.40	2.92	2.02	3.01
Conemaugh	54.93	26.30	8.12	0.44	2.92	1.45	5.84

\* others include Ti, Mg, P, S oxides.

Table 2. Si/Al and Na/Al molar ratios of treated fly ashes containing faujasite, and commercial zeolite (UOP ZY-54).

	UOP ZY-54	Goudey Ash	Eddystone Ash	Conemiaugh Ash
Si/Al	2.64 $\pm$ 0.02	1.19 $\pm$ 0.07	1.23 $\pm$ 0.09	1.21 $\pm$ 0.07
Na/Al	1.14 $\pm$ 0.07	1.00 $\pm$ 0.10	0.99 $\pm$ 0.30	0.92 $\pm$ 0.12

Table 3. Lattice Parameter,  $a_0$ , and Si/Al molar ratio of treated fly ashes containing faujasite, and commercial zeolite (UOP ZY-54).

	UOP ZY-54	Goudey Ash	Eddystone Ash	Conemiaugh Ash	Eddystone Ash *
$a_0$ (Å)	24.77	24.99	25.03	24.95	25.10
Si/Al**	2.17	1.23	1.14	1.30	1.04

\*The treated Eddystone I ash obtained from the low-temperature process without fusion.

\*\* The Si/Al ratio is estimated from Ref. 17.

Table 4. Ion exchange capacity (millieq/g) of treated fly ashes containing faujasite or zeolite P, and commercial zeolites with respect to 0.1 N of  $\text{Cs}^+$  ion.

UOP X-60	UOP ZY-54	Faujasite (Goudey)	Faujasite (Eddystone)	Faujasite (Conembaugh)	Zeolite P (Eddystone)
2.13	1.86	1.60	1.51	1.61	0.15

millieq/g = exchanged amount of  $10^{-3}$  mole sodium ion per gram of treated fly ashes or commercial zeolite.

Table 5. Ion exchange capacity (millieq/g) of treated fly ashes containing faujasite or zeolite P, and commercial zeolites with respect to 0.1 N of  $\text{Co}^{2+}$  ion.

UOP 4A	UOP X-60	UOP ZY-54	Faujasite (Goudey)	Faujasite (Eddystone)	Faujasite (Conembaugh)	Zeolite P (Eddystone)
3.62	3.47	1.75	2.46	2.30	2.74	0.66

millieq/g = exchanged amount of  $10^{-3}$  mole sodium ion per gram of treated fly ashes or commercial zeolite.

Table 6. Specific surface area ( $\text{m}^2/\text{g}$ ) of treated fly ashes with/without fusion and commercial zeolites (UOP ZY-54, UOP4A).

Samples	Specific surface area ( $\text{m}^2/\text{g}$ )
UOP ZY-54	950
UOP4A	800
Faujasite (Eddystone ash I)*	Solution : 100
Zeolite A (Eddystone ash I)*	Solution : 74.78
Faujasite (Goudey)	Supernatant : 654.6 Solution : 511
Faujasite (Eddystone II)	Solution : 272.9
Faujasite (Conembaugh)	Supernatant : 640.2 Solution : 445
Zeolite P (Eddystone II)	Solution : 54.4

\* Zeolites converted from Eddystone ash I without fusion pretreatment.

Table 7. Concentration of Si, Al and Na in solution I and II, prepared from Conembaugh ash.

	Si (ppm)	Al (ppm)	Na (ppm)
Solution I	2740	528	46000
Solution II	572	161.2	12000
Solution III	167	92	2810

Table 8. Chemical compositions of as-received Conemahaugh ash and the precipitates with different morphologies shown in Fig. 22.

Elements* (atom%)	Fly Ash (Conemahaugh)	MCM-41	Fibril	Particle	Chunk #
Si	19.54	31.21	31.86	32.29	28.64
Al	11.04	2.33	1.53	1.11	4.90
Fe	6.66	0.28	0.15	0.04	0.17
Na	0.31	ND**	ND**	ND**	0.46
K	1.08	0.12	0.05	0.05	0.28
Ca	0.45	0.12	0.07	0.10	0.14
O	60.93	67.03	66.33	66.42	65.41

\* The elements are assumed to exist as oxides,  $\text{SiO}_2$ ,  $\text{Al}_2\text{O}_3$ ,  $\text{Fe}_2\text{O}_3$ ,  $\text{Na}_2\text{O}$ ,  $\text{K}_2\text{O}$ ,  $\text{CaO}$

\*\* ND : not detectable

# Chunk was not shown in Fig. 22.

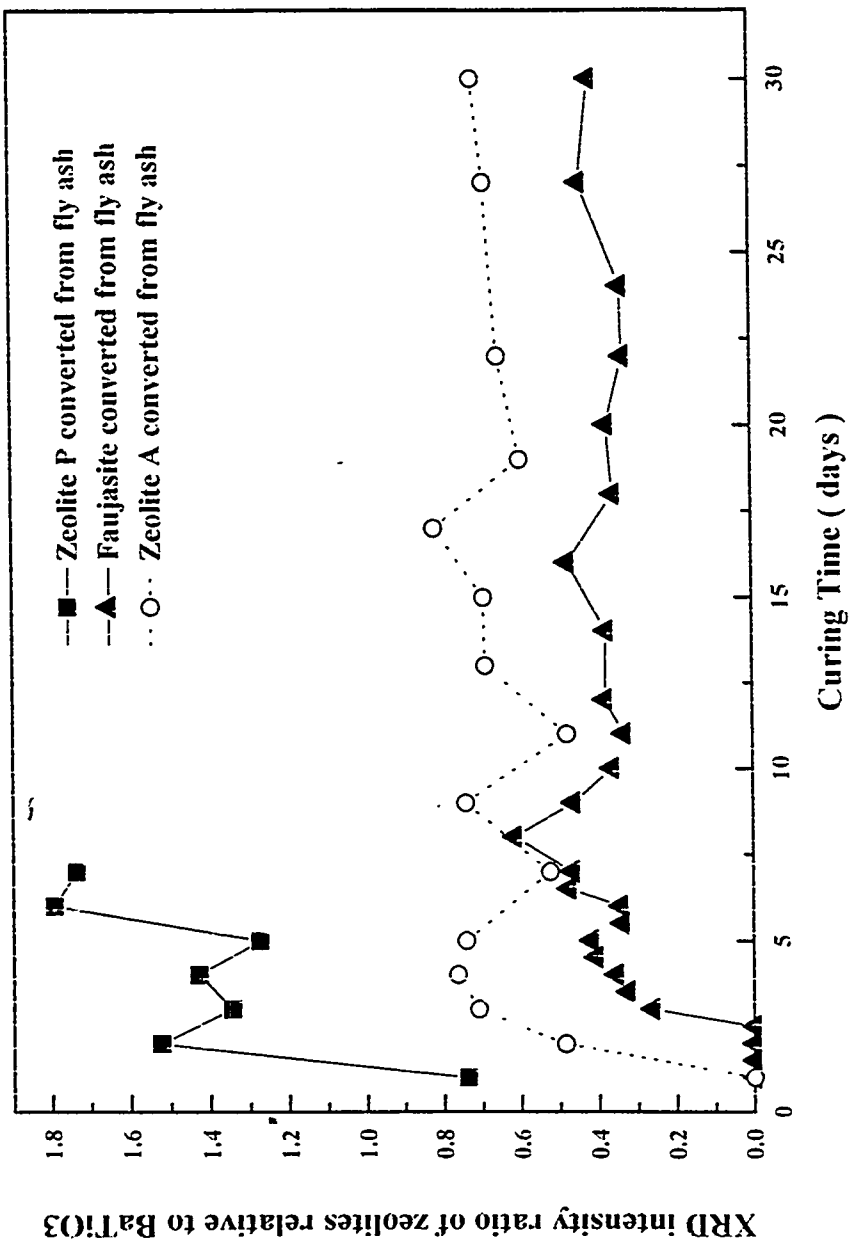


Figure 1. XRD intensity ratio of generated zeolites related to  $\text{BaTiO}_3$  as a function of curing time.

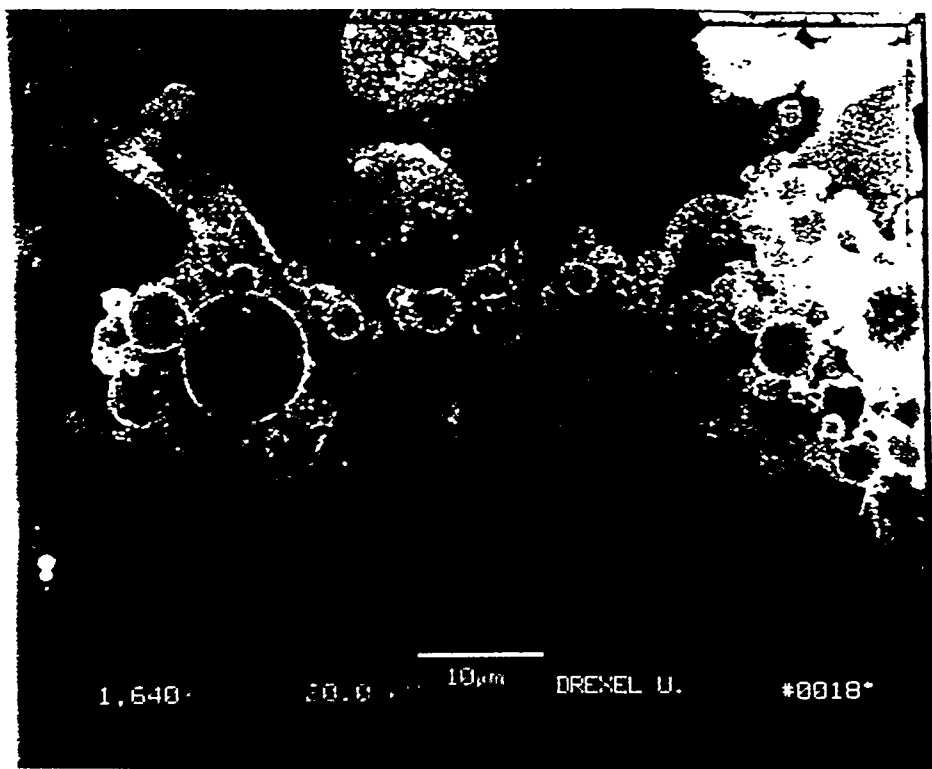


Figure 2. SEM micrograph of as-received Eddystone ash.

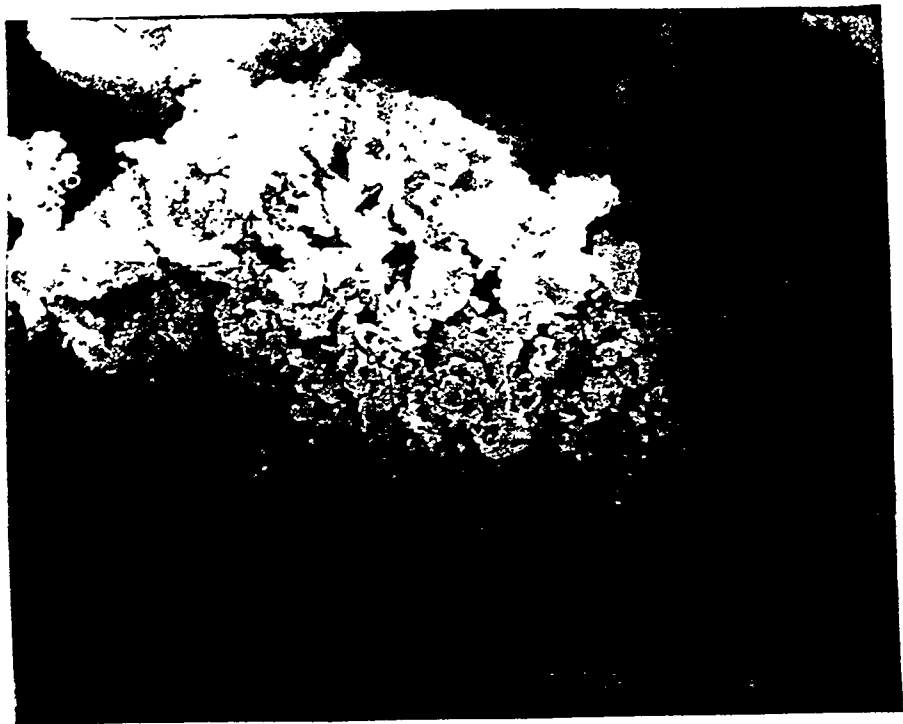


Figure 3. SEM micrograph of treated Eddystone ash (I) containing faujasites.



Figure 4. SEM micrograph of treated Eddystone ash (I) containing zeolite A.

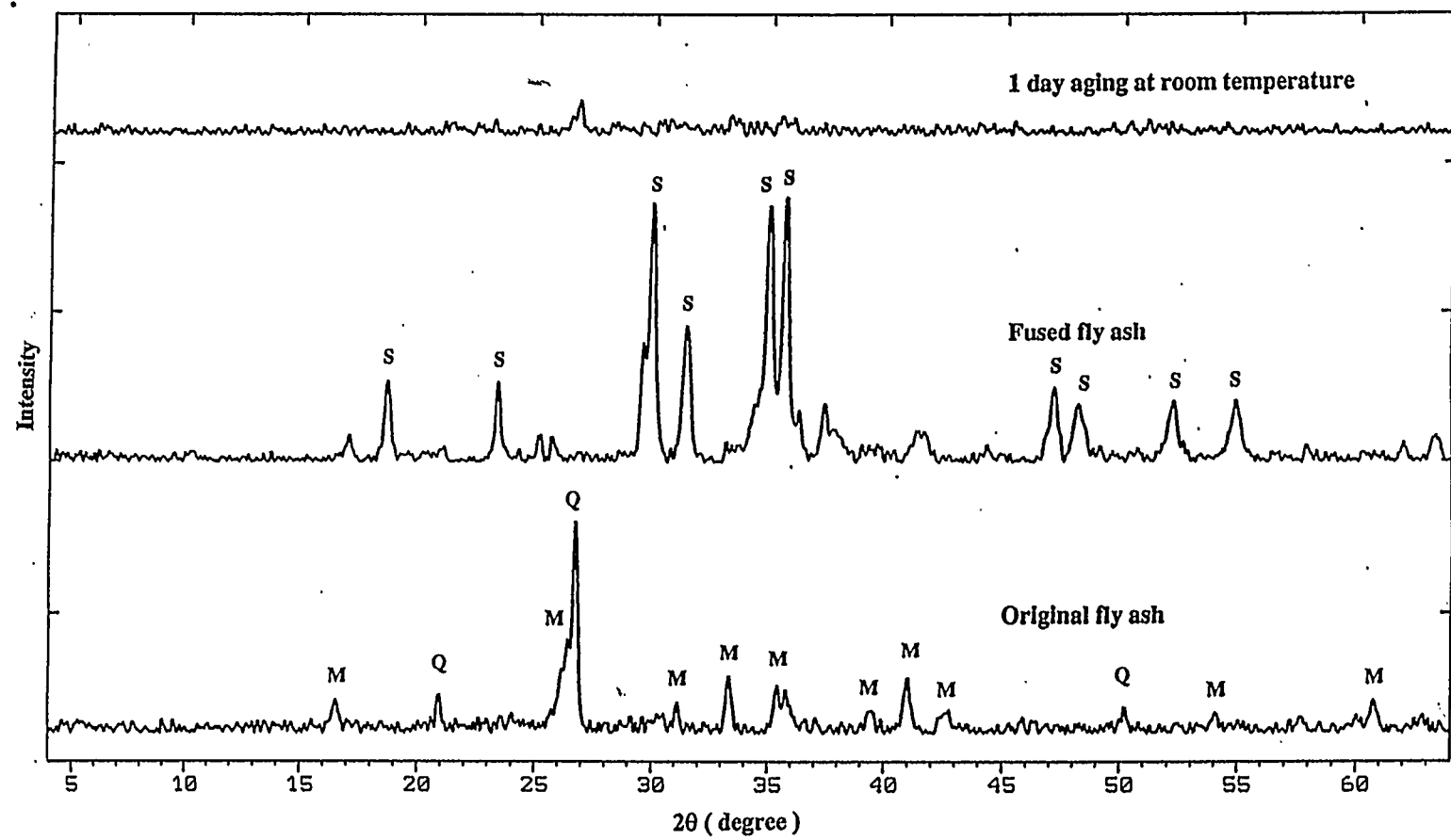


Figure 5. XRD pattern of as-received fly ash, fused fly ash, and the sediment of the fused fly ash solution after 1 day of aging. M : mullite; Q : quartz; S : sodium silicate.

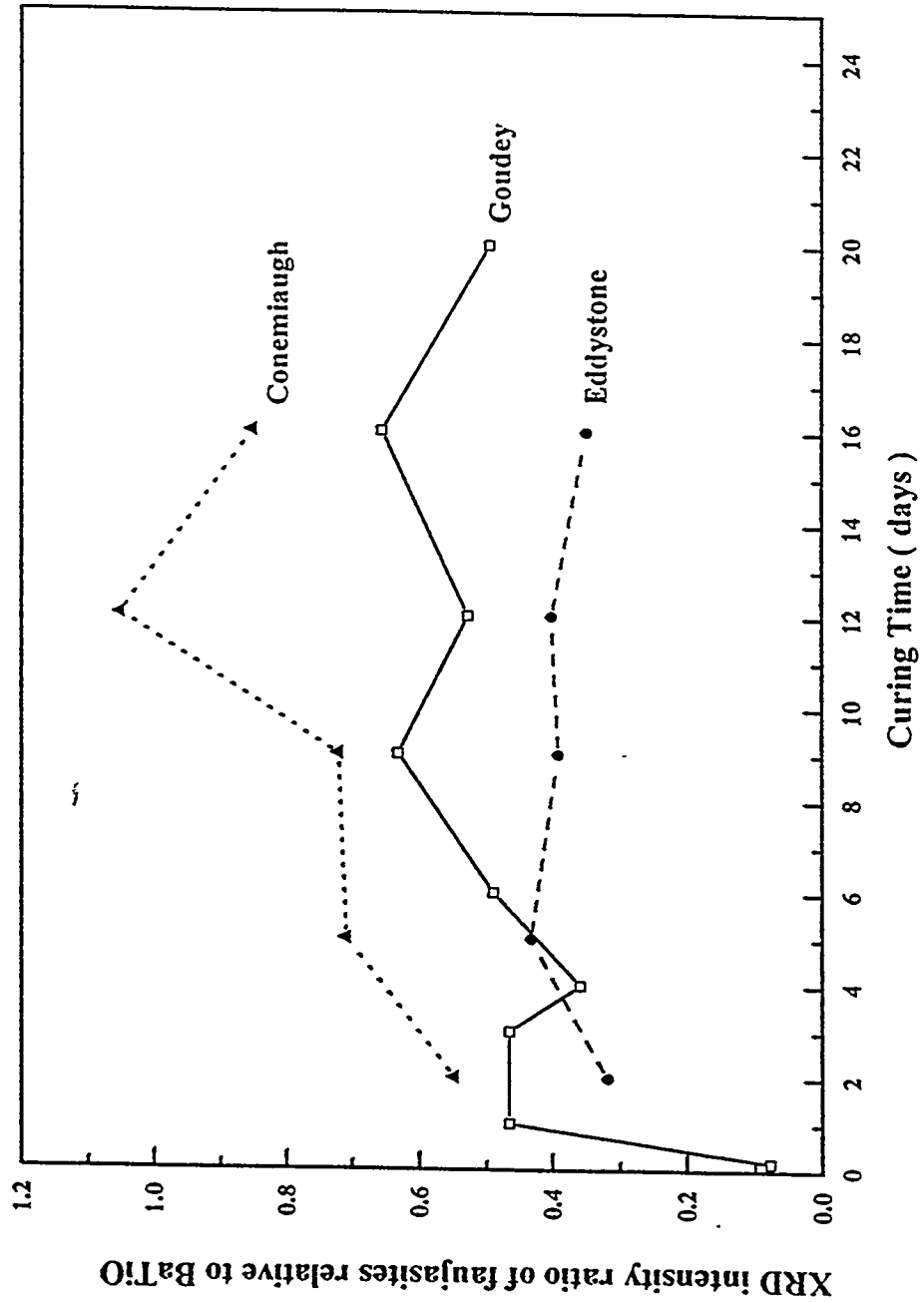


Figure 6. The XRD intensity ratio of the produced fayujasites from fused fly ashes relative to  $\text{BaTiO}_3$  as a function of curing time.

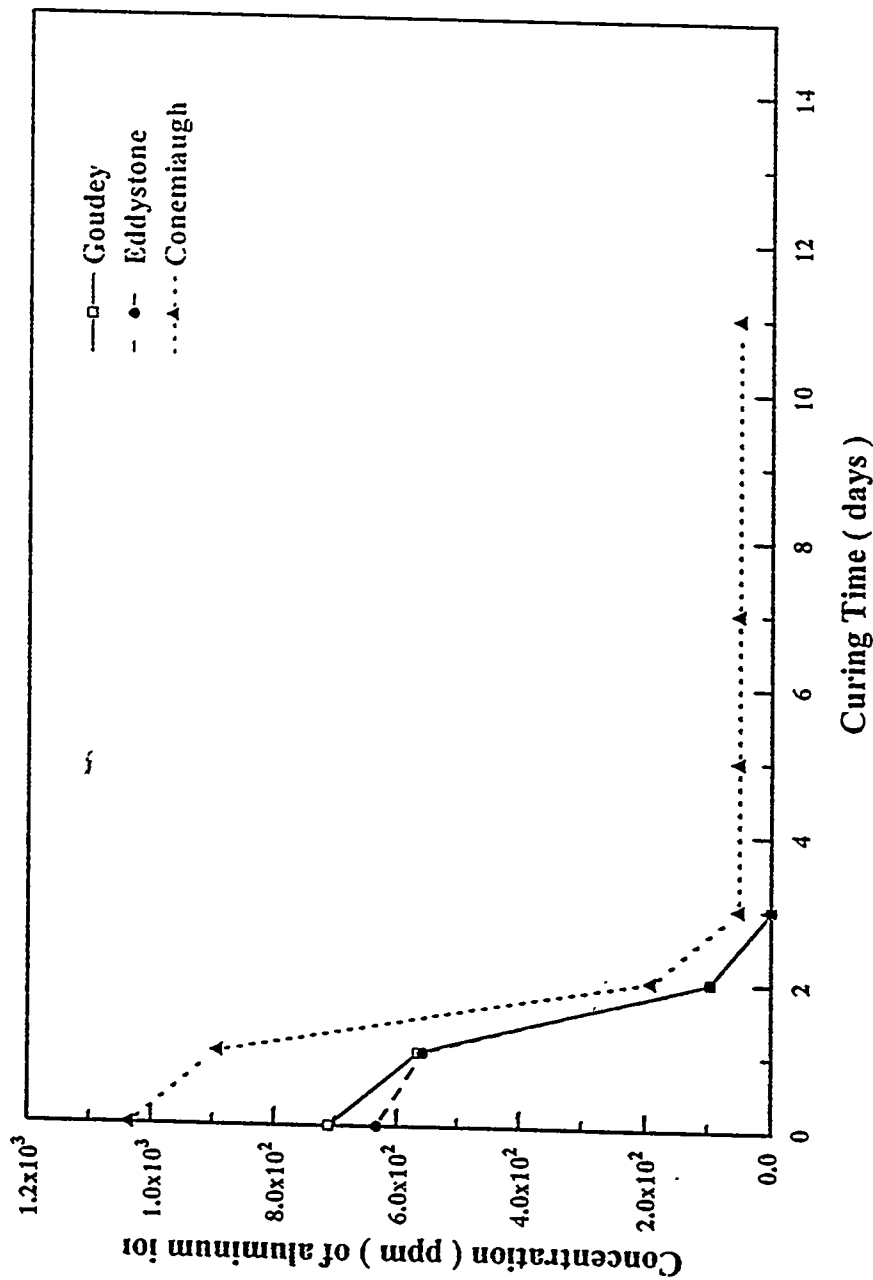


Figure 7. Concentration of aluminum ions in the curing solutions as a function of curing time for three ashes.

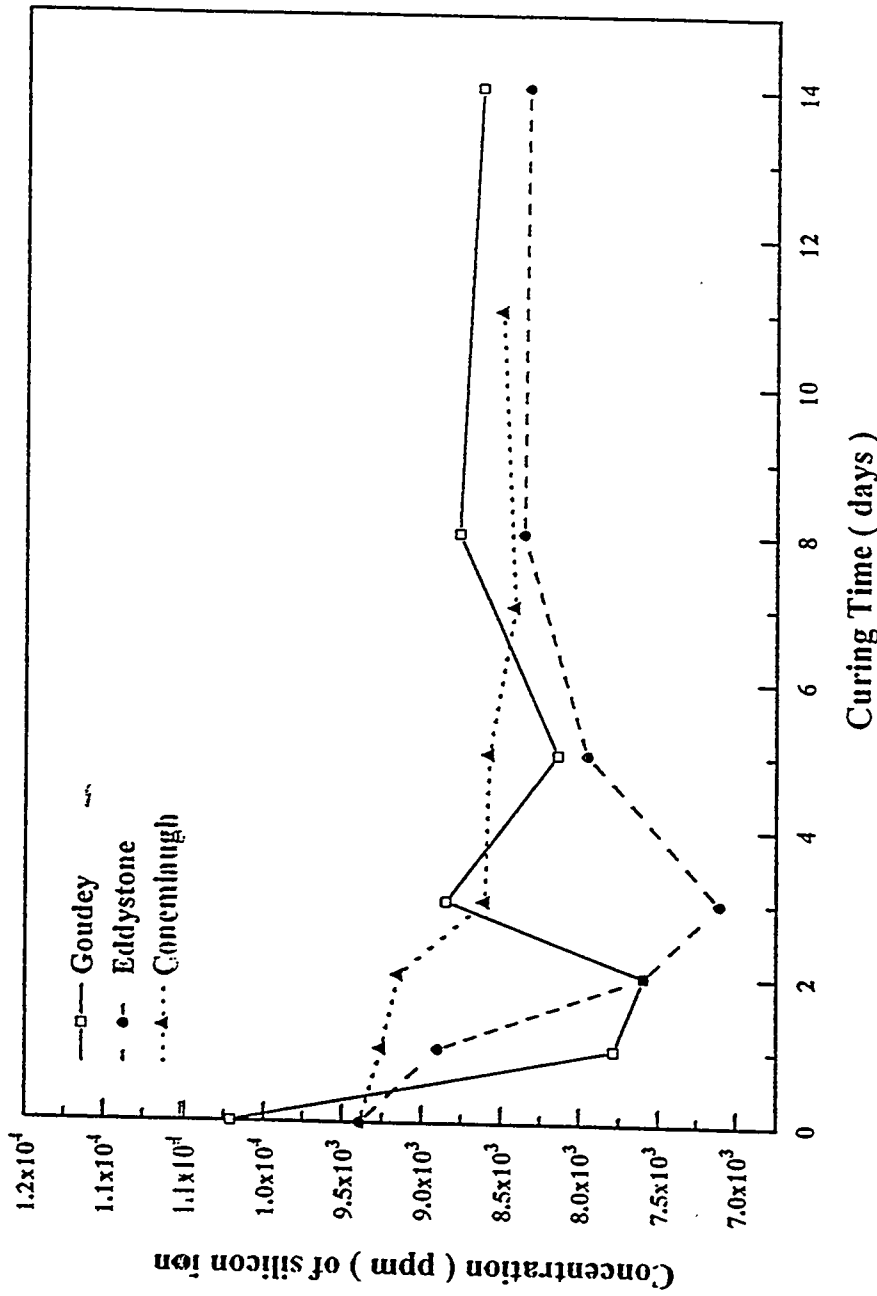


Figure 8. Concentration of silicon ions in the curing solutions as a function of curing time for three ashes.

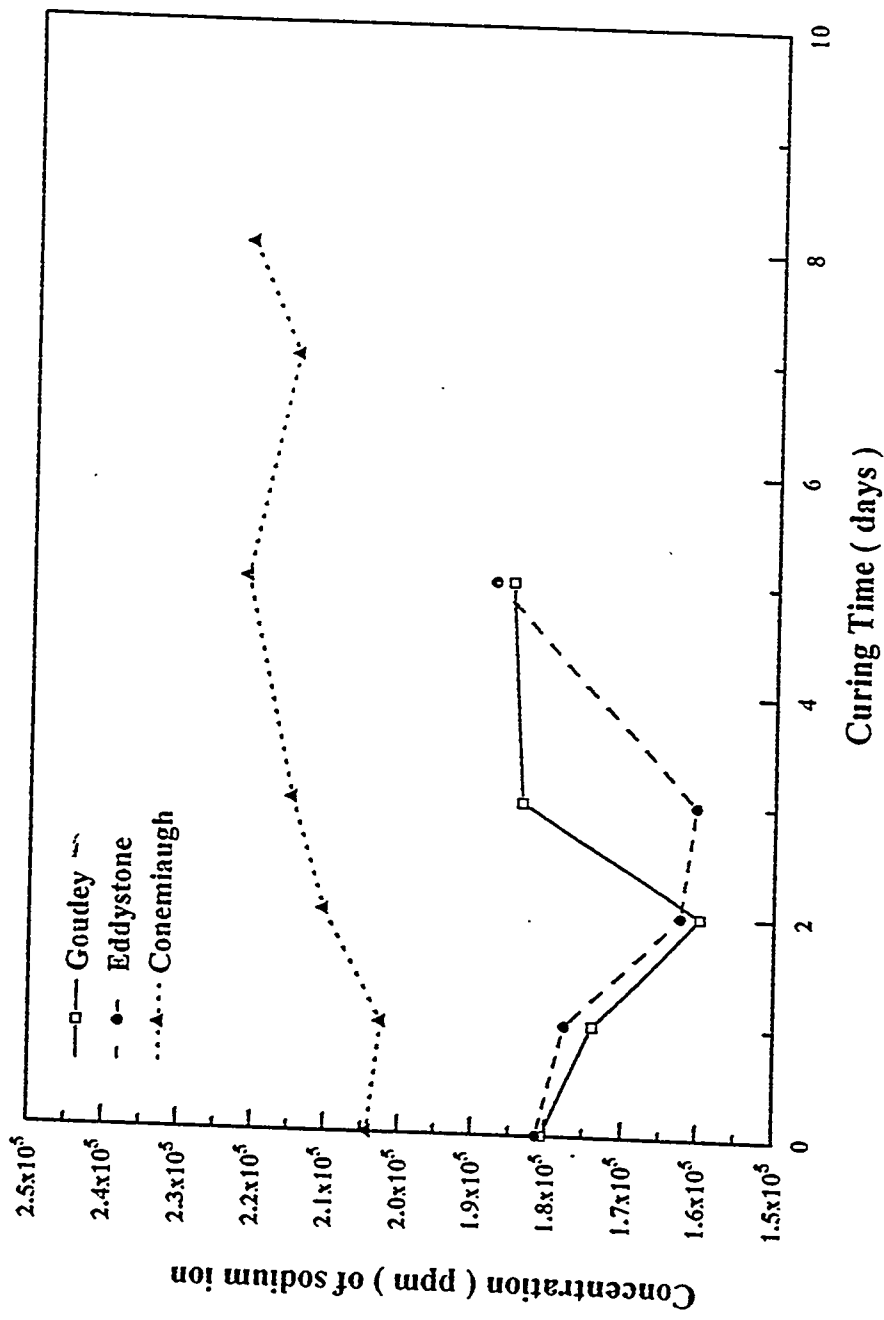


Figure 9. Concentration of sodium ions in the curing solutions as a function of curing time for three ashes.

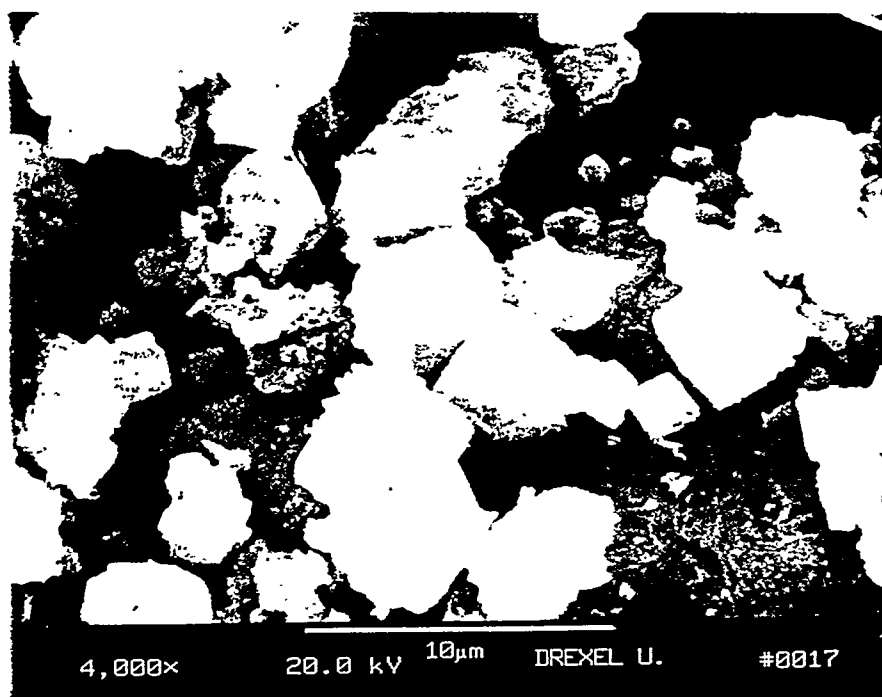


Figure 10. SEM micrograph of the generated faujasite from Conembiaugh ash.

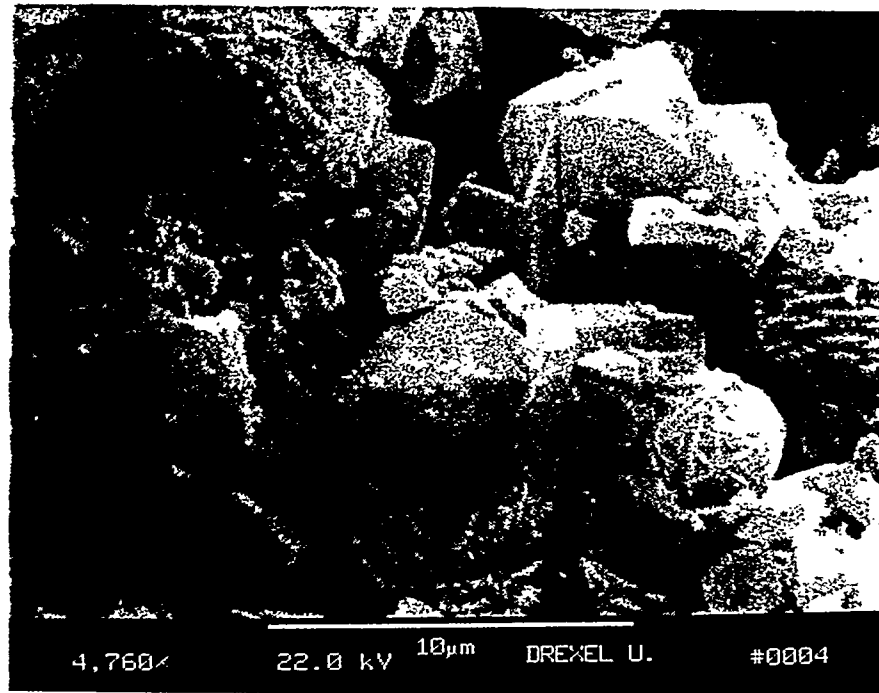


Figure 11. SEM micrograph of the generated faujasite from the supernatant of the fused Conemaugh ash solution.

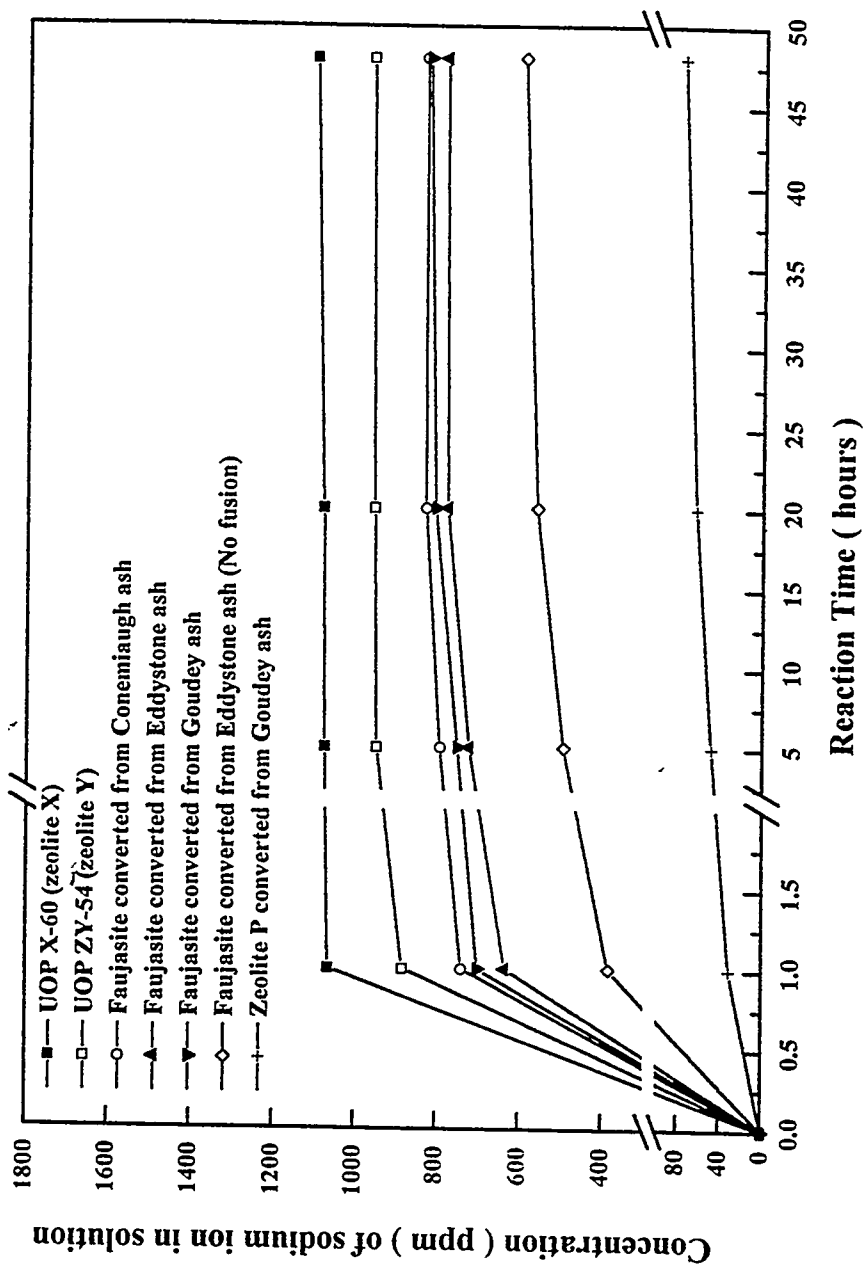
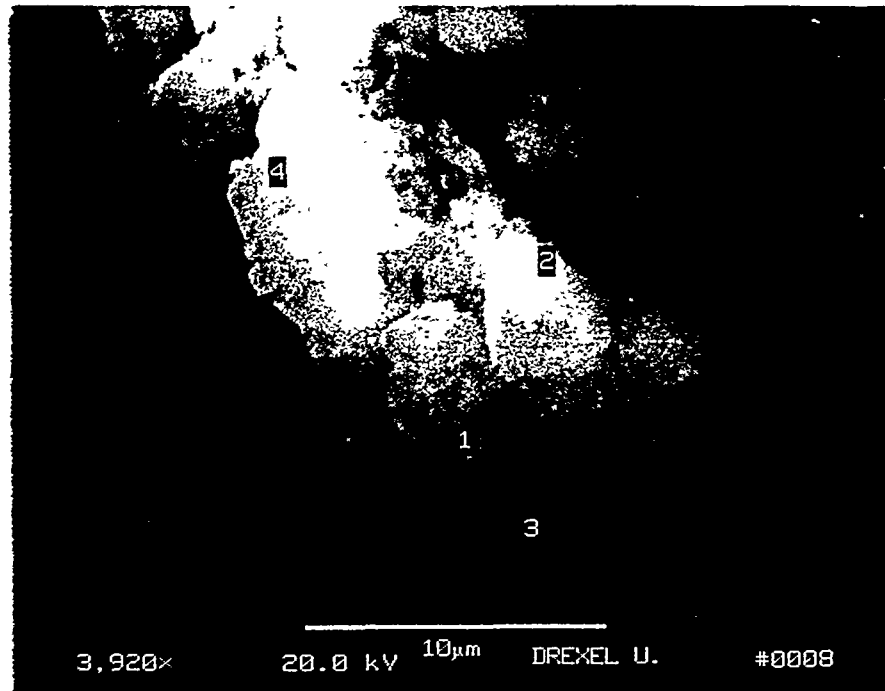


Figure 12. Concentration of sodium ion in the solution of 40 ml of 0.1 N cesium chloride and 0.9 g of treated fly ashes containing faujasite by fusion, treated fly ash without fusion treatment, or commercial zeolites as a function of reaction time.



SEM-EDXS Measurement of Faujasite Converted From Conemaugh Ash

#	# 1	# 2	# 3	# 4
Ion Exchange Capacity (millieq/g )	3.70	1.52	3.62	1.62
Si/Al molar ratio	1.28	1.27	1.33	1.17

Figure 13. SEM micrograph of treated fly ash containing faujasite, and the Si/Al ratio and Cs<sup>+</sup> ion exchange capacity at different locations measured by EDXS.

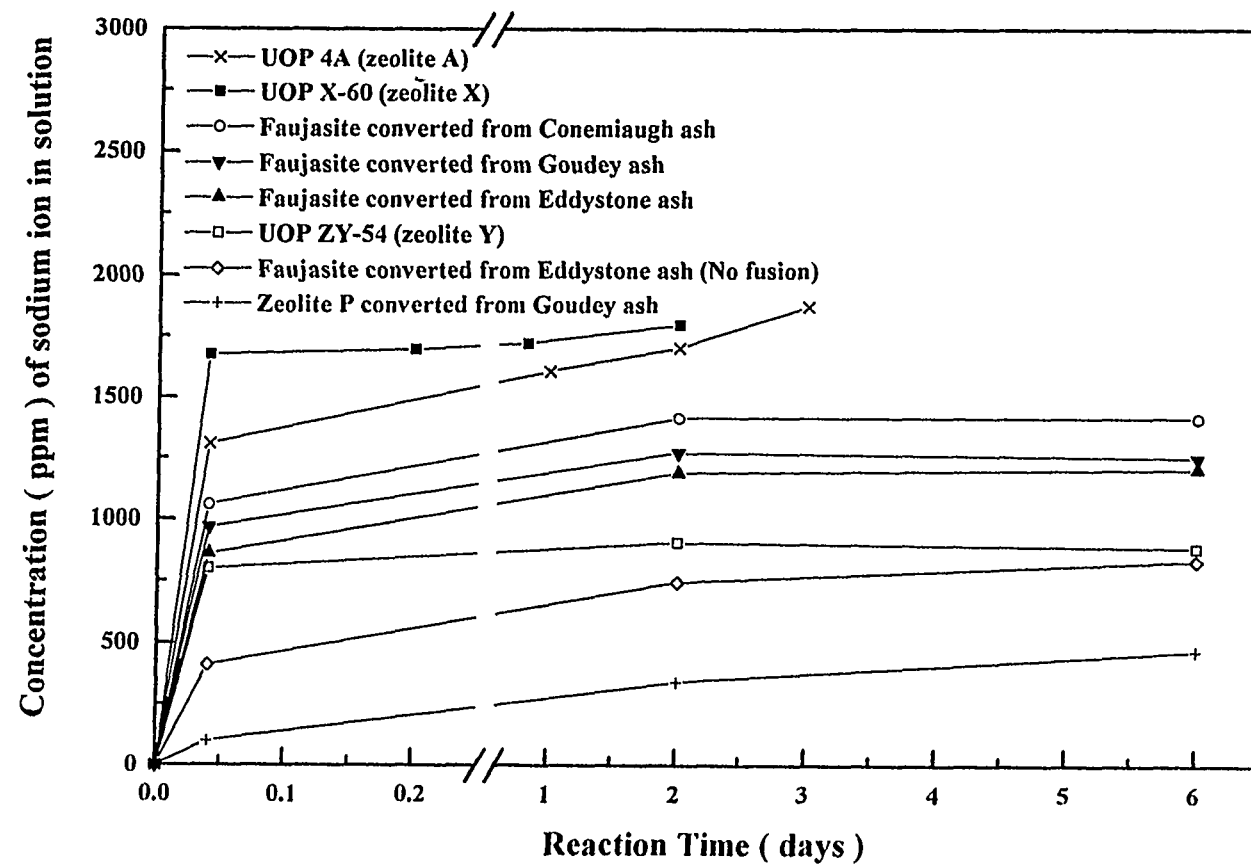
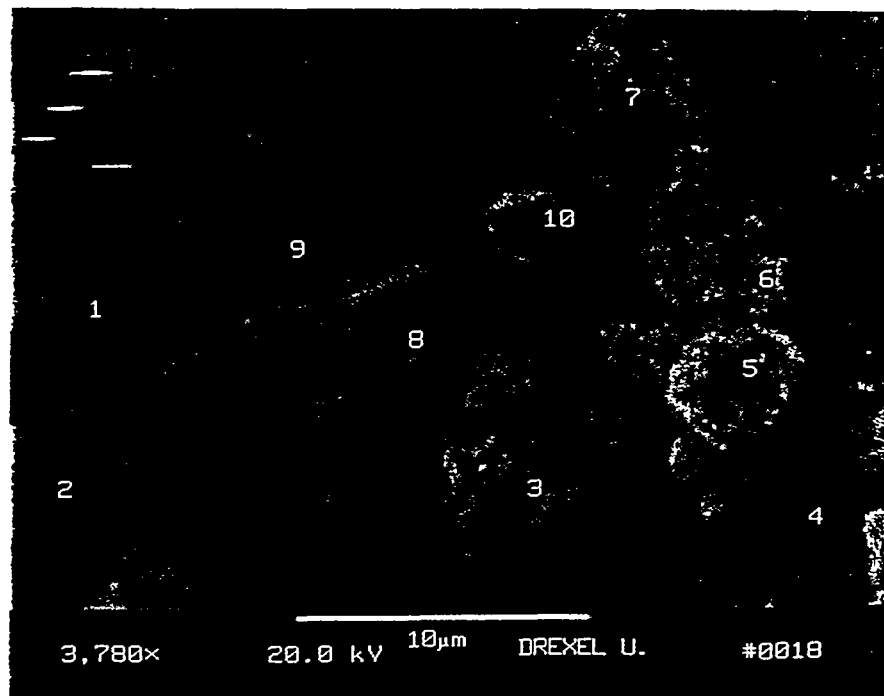


Figure 14. Concentration of sodium ion in the solution of 40 ml of 0.1 N cobalt chloride and 0.9 g of treated fly ashes containing faujasite by fusion or commercial zeolites as a function of reaction time.



SEM-EDXS Measurement of Faujasite Converted From Conemaugh Ash

A	# 1	# 2	# 3	# 4	# 5	# 6	# 7	# 8	# 9	# 10	Ave
Ion Exchange Capacity with 0.1 N $\text{Co}^{2+}$ (millieq/g )	4.59	3.08	3.48	3.92	2.78	3.89	4.46	1.88	2.70	4.07	3.49
Si/Al molar ratio	1.58	2.40	1.76	1.85	1.68	2.46	1.95	1.89	4.20	2.29	2.21

Figure 15. SEM micrograph of treated fly ash containing faujasite, and the Si/Al ratio and  $\text{Co}^{2+}$  ion exchange capacity at different locations measured by EDXS.

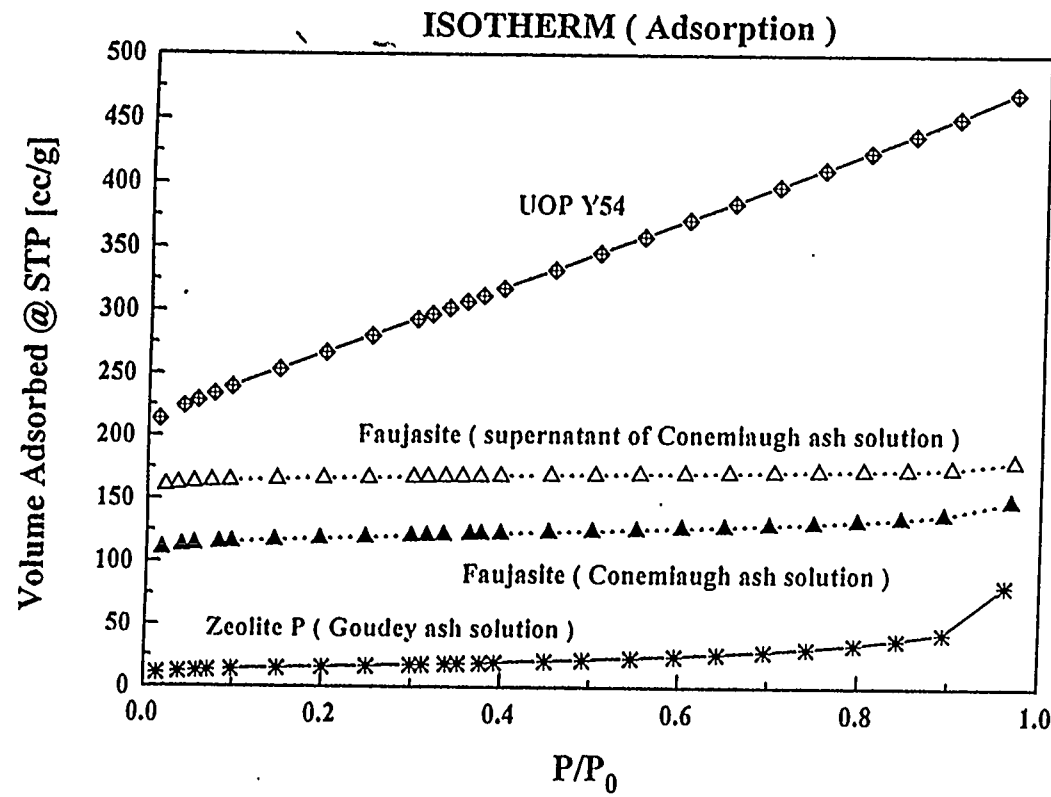


Figure 16. Nitrogen gas adsorption isotherms of treated Conemaugh ash containing faujasite or zeolite P by hydrothermal procedure (1), treated Conemaugh ash containing faujasite by hydrothermal procedure (2), and commercial zeolite (UOP ZY-54).

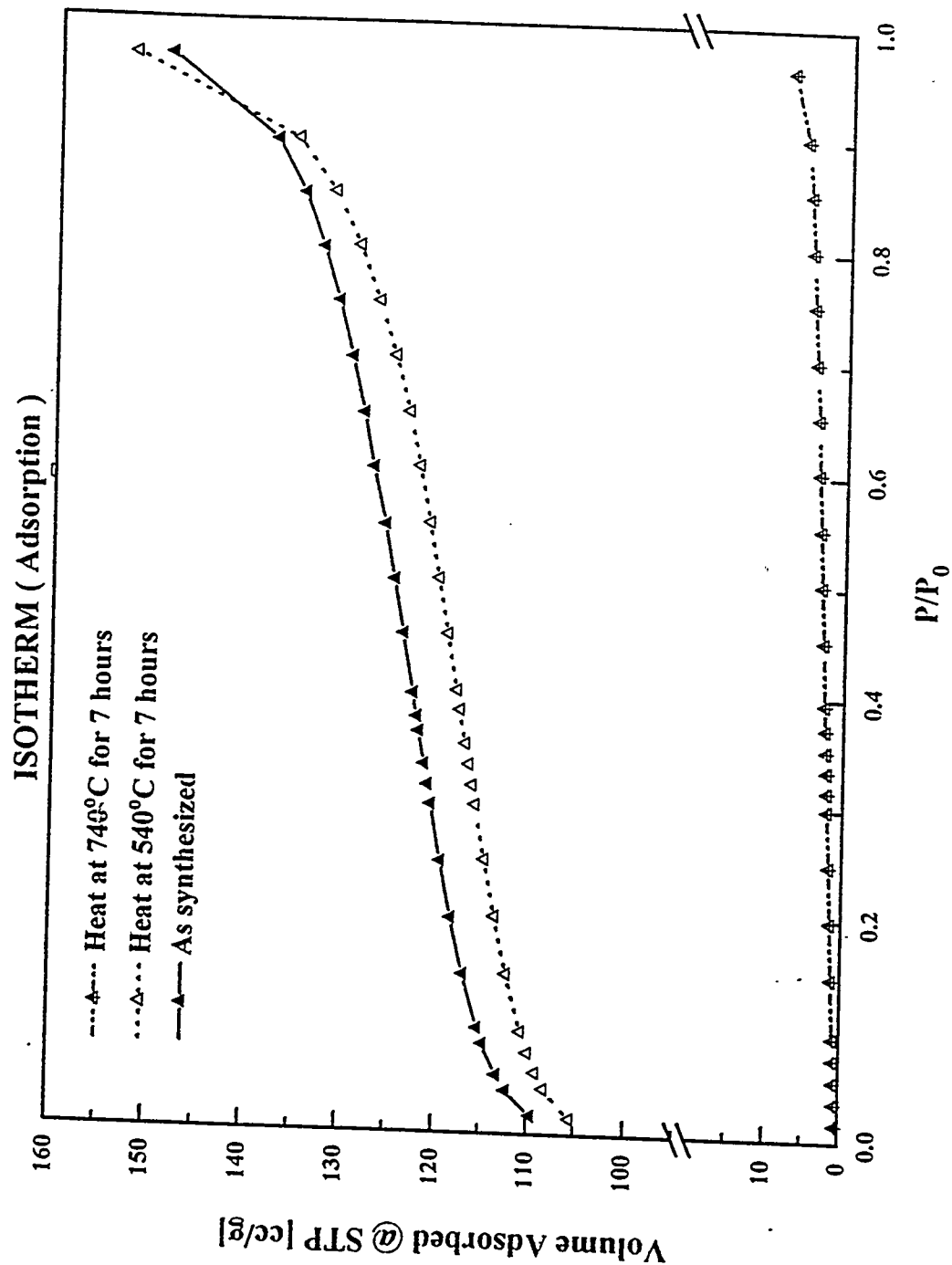


Figure 17. Nitrogen gas adsorption isotherms of treated fly ash containing fayjasites after heat treatment at different temperatures.

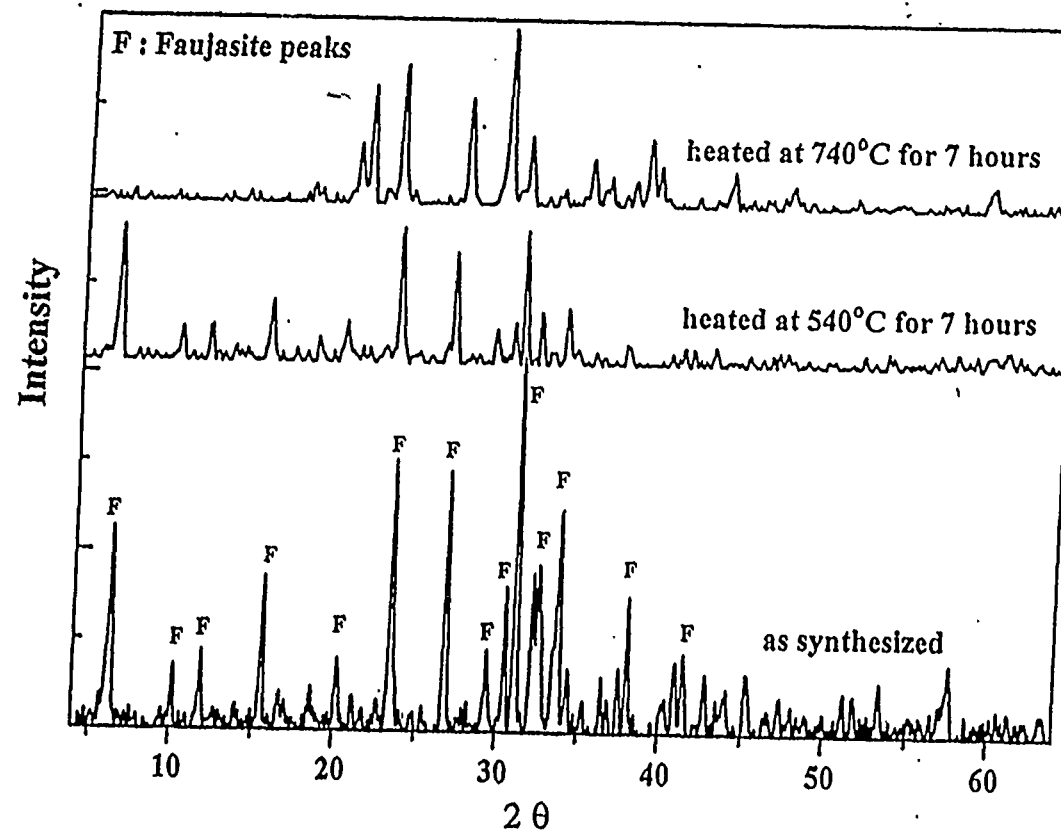


Figure 18. XRD patterns of treated fly ash containing faujasites after heat treatment at different temperatures.

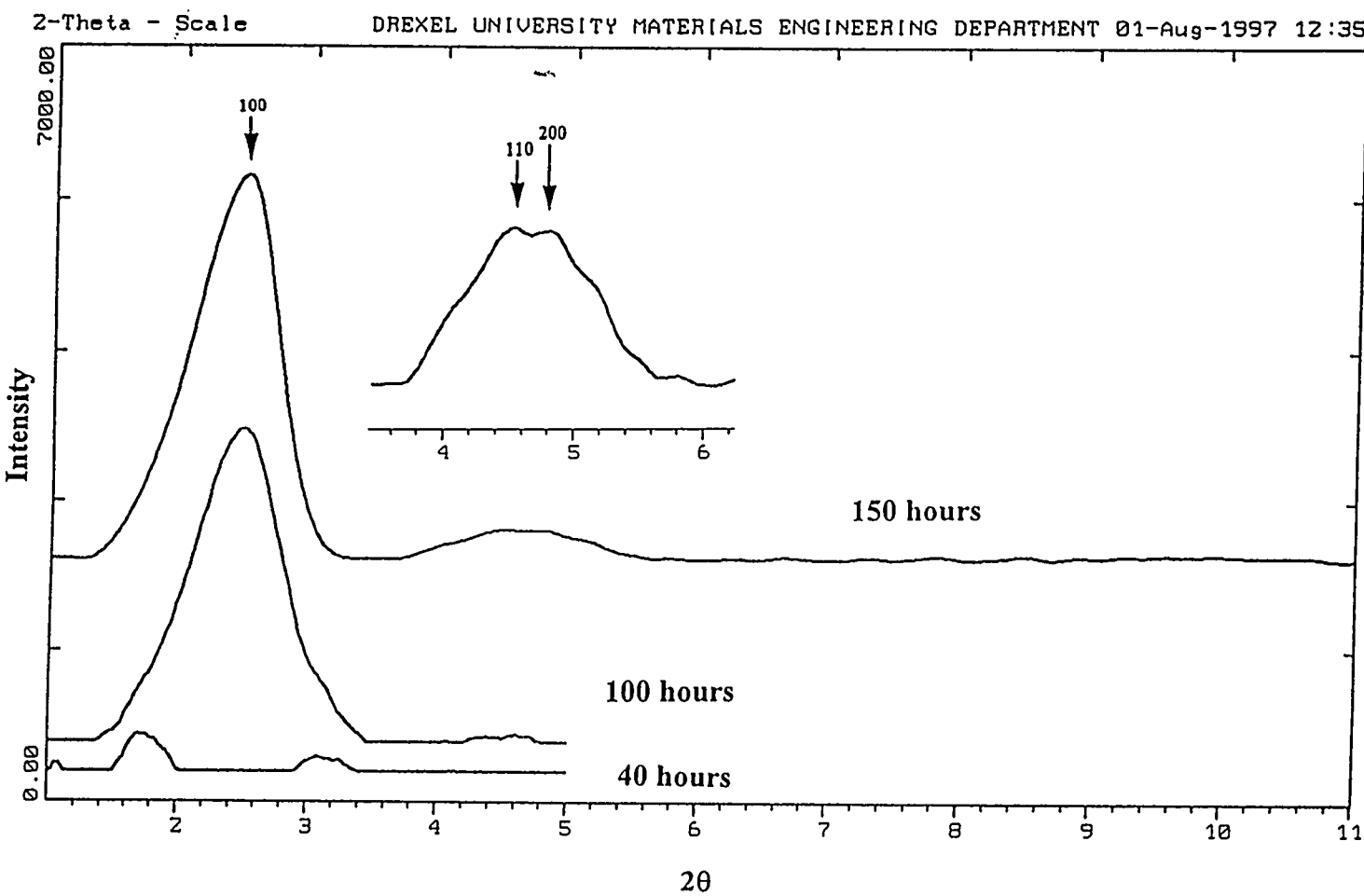


Figure 19. The XRD pattern of calcined aluminosilicate obtained from the supernatant of the solution II after various curing times at 115°C.

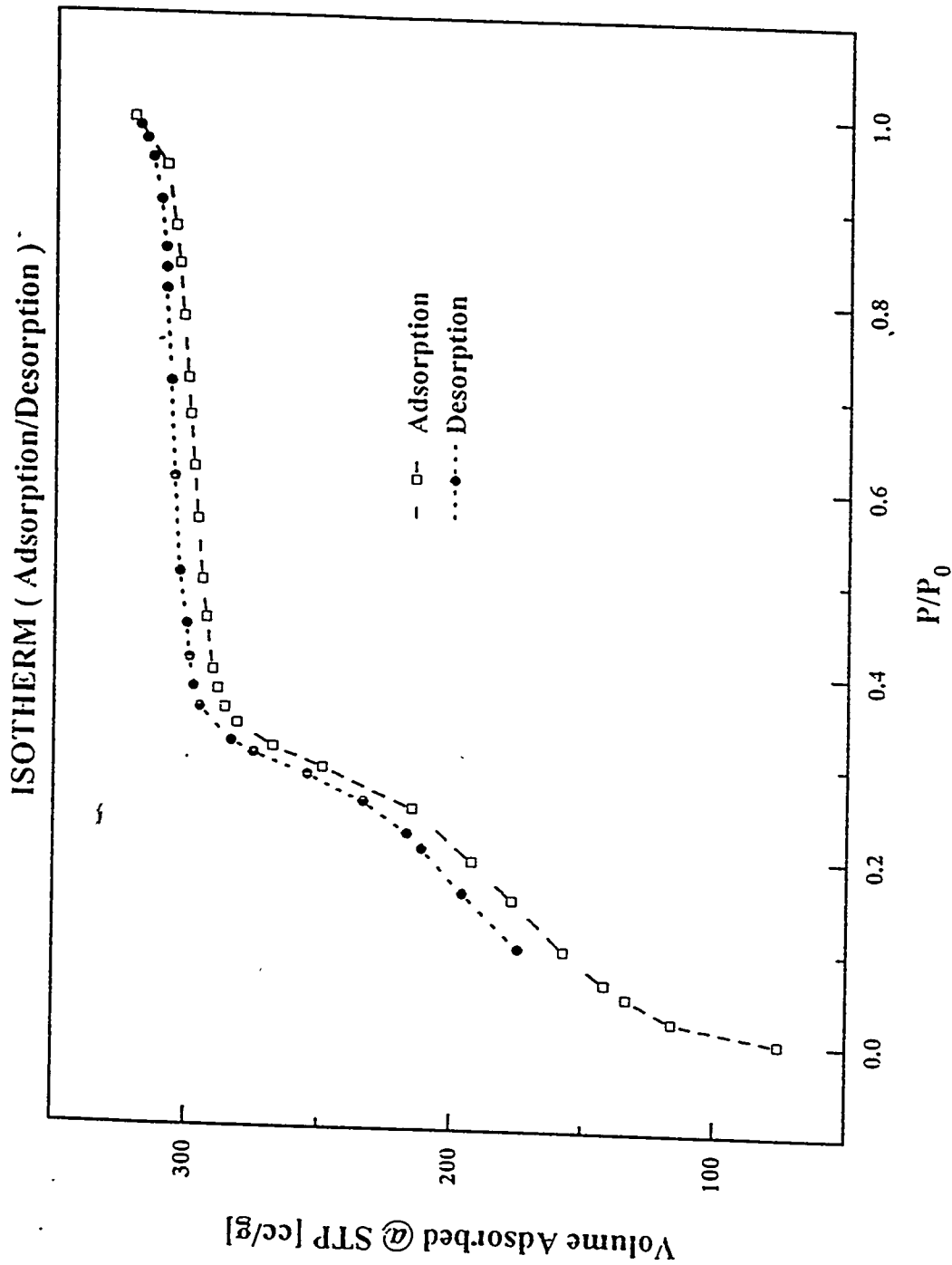


Figure 20. The nitrogen gas adsorption/desorption isotherms for the MCM-41 phase obtained from solution II prepared from Connemara ash and cured at 115°C for 150 hours.

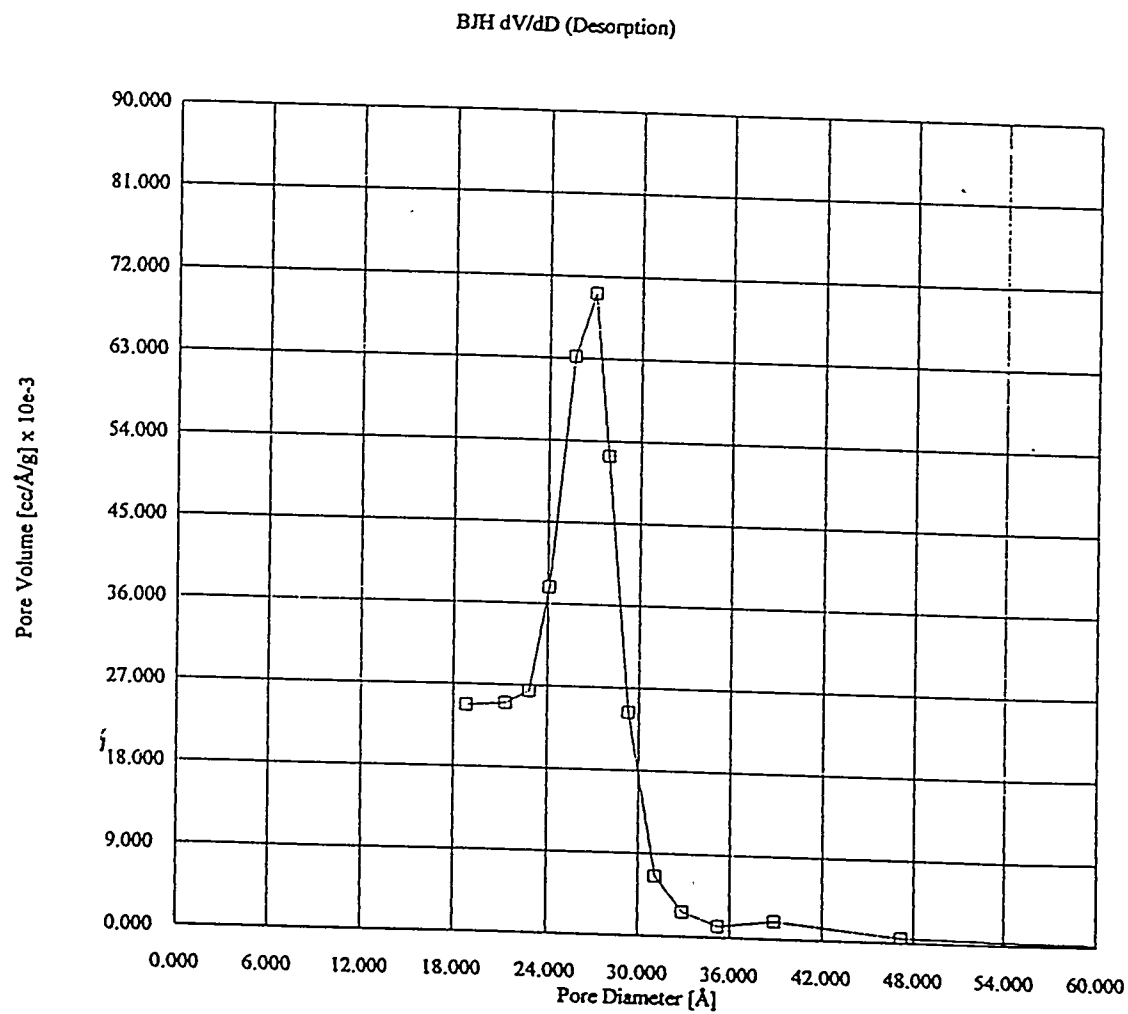


Figure 21. The pore size distribution the MCM-41 phase obtained from solution II prepared from Conemiaugh ash and cured at 115°C for 150 hours.

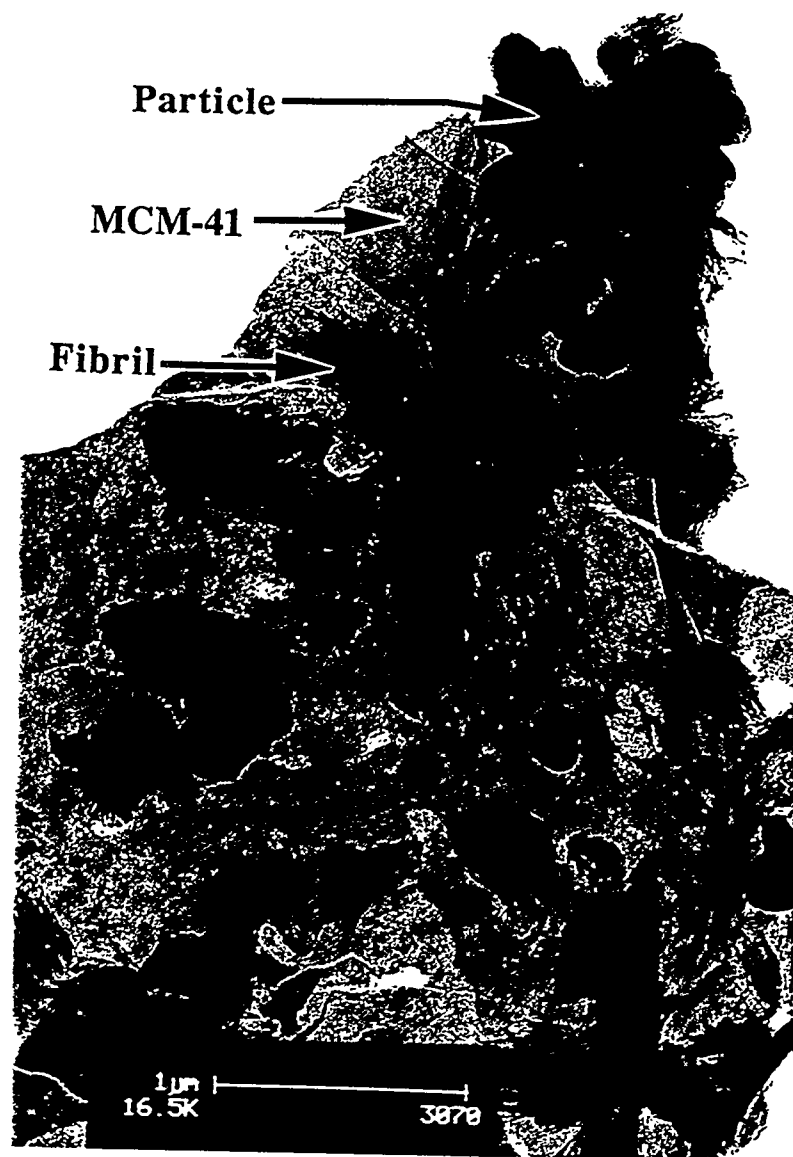


Figure 22. The TEM micrograph of the MCM-41 phase obtained from solution II prepared from Conemaha ash and cured at 115°C for 150 hours. A large piece of plate region is embedded with particles and fibrils.

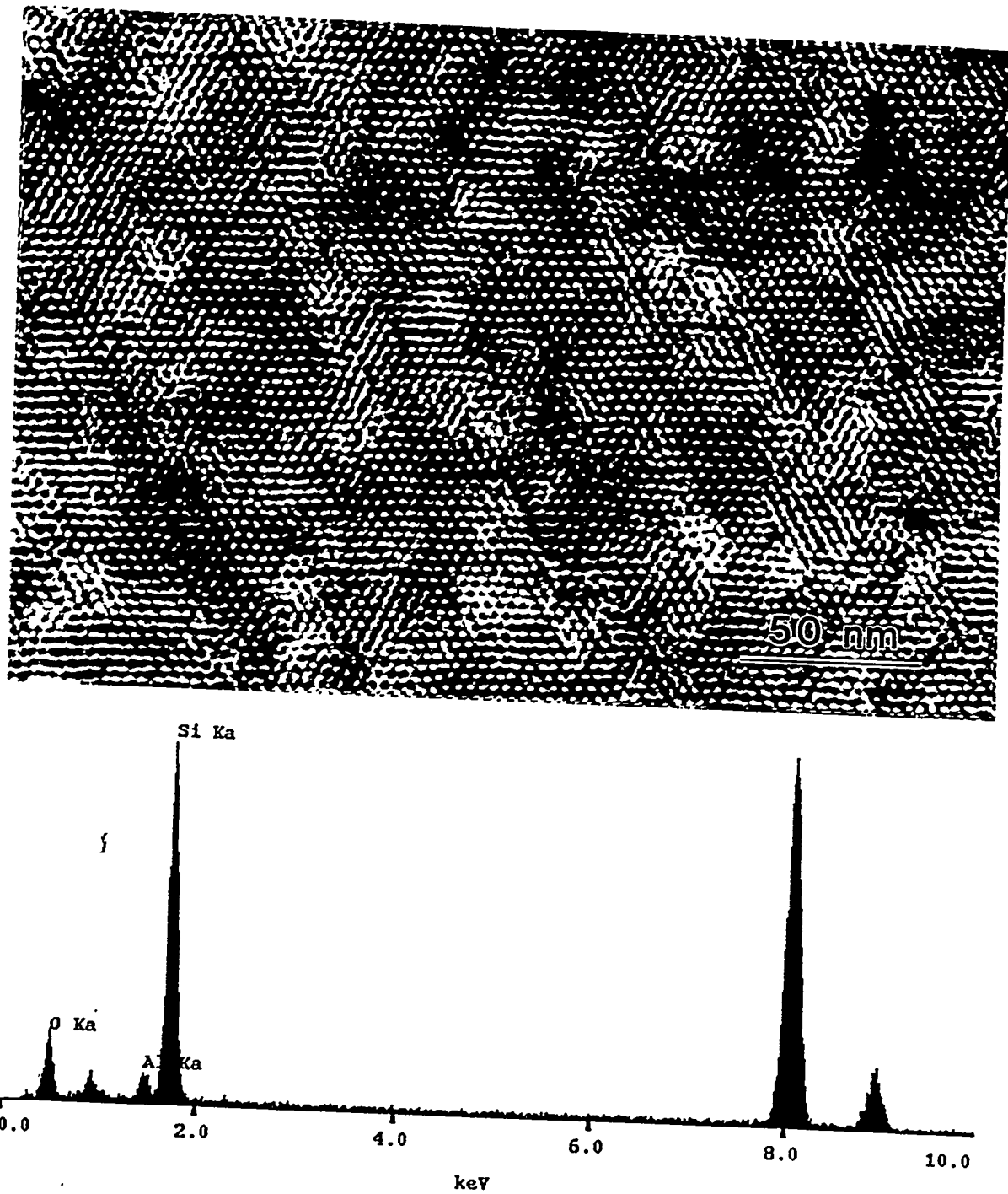


Figure 23. The TEM micrograph of the plate regions shown in Fig. 7.56 at a higher magnification. The pores are orderly arranged in a hexagonal pattern indicating MCM-41 structure existence in the plate region.

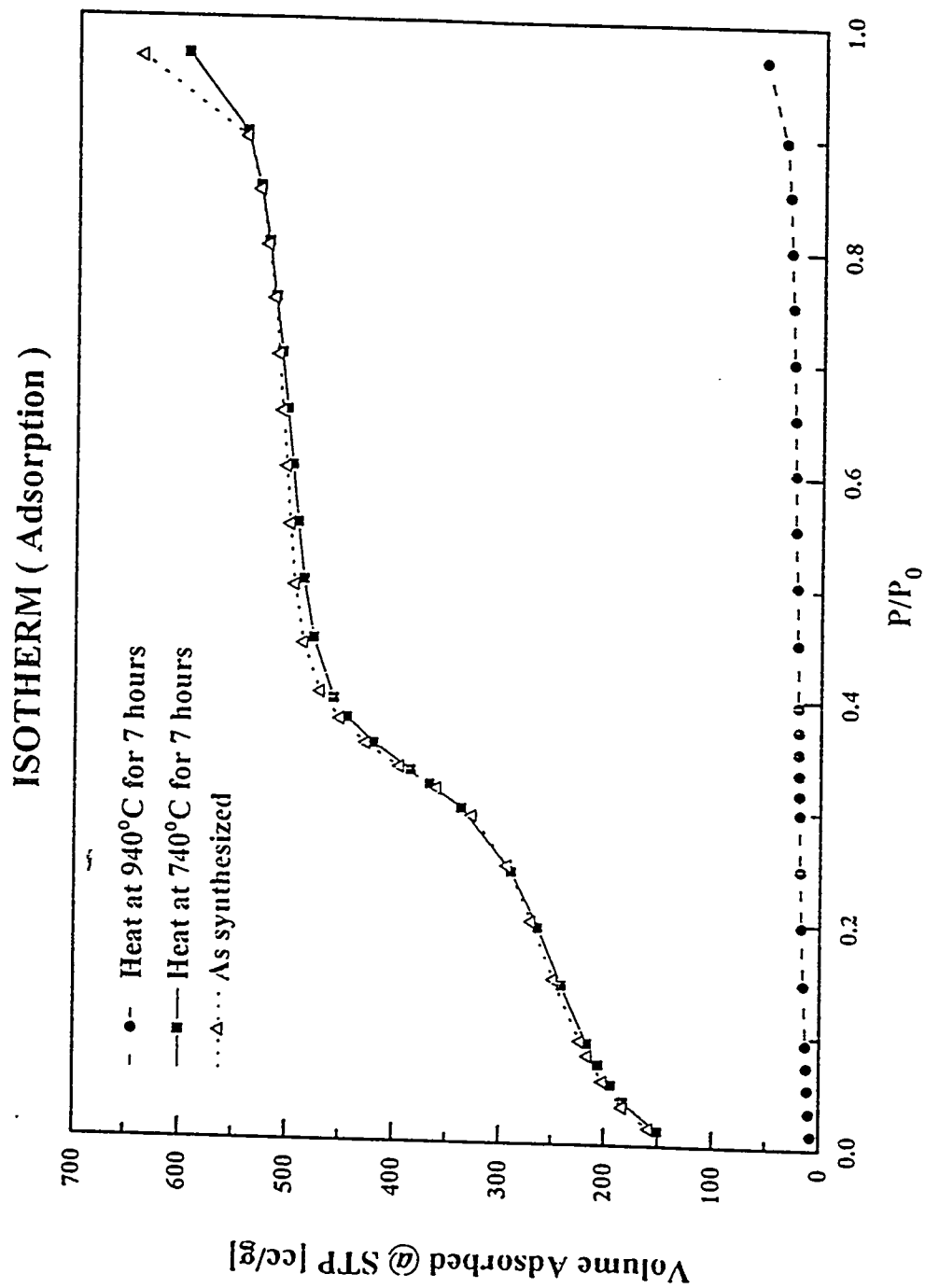


Figure 24. The nitrogen gas adsorption isotherms of MCM-41 materials converted from fly ash after heat treatment at various temperatures for 7 hours.

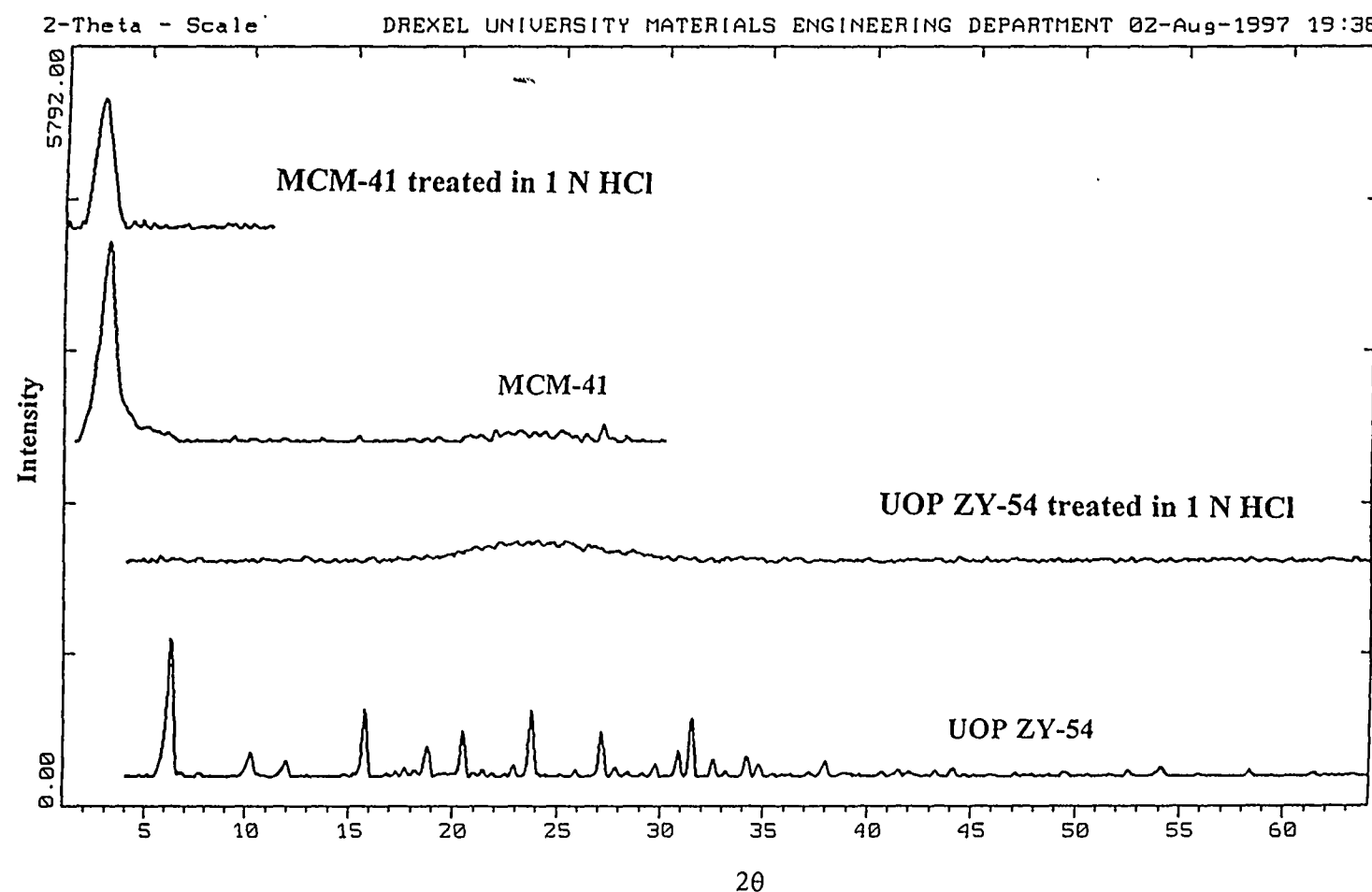


Figure 25. The XRD pattern of MCM-41 materials converted from fly ash and commercial zeolite (UOP ZY-54) after soaking in 1 N of hydrogen chloride solution for 1 day.